JOURNAL OF MATERIALS SCIENCE 33 (1998) 1959–1980

Review
Reinforced cast metals
Part II *Evolution of the interface*

R. ASTHANA
Manufacturing Engineering, Technology Department, University of Wisconsin-Stout, Menomonie, WI 54751, USA
E-mail: asthanar@uwstout.edu

Interface evolution in metal-matrix composites is a thermodynamic necessity and interface design a kinetics challenge. The synergistic interaction between processing science and surface engineering has led to considerable progress in understanding, modelling and tailoring the fibre–matrix interface at the microstructural, crystallographic and atomic levels. The chemical, morphological, crystallographic and thermoelastic compatibilities between the fibre and the matrix influence the interfacial adhesion strength. This article examines the role of material properties and fabrication conditions in chemical interactions between the fibre and the matrix in metal-matrix composites synthesized using the solidification and casting techniques. © *1998 Chapman & Hall*

1. Introduction

Interfaces constitute an important microstructural feature of composite materials. They are transition zones of finite dimensions at the boundary between the fibre and the matrix where compositional and structural discontinuities can occur over distances varying from an atomic monolayer to over five orders of magnitude in thickness. As the inherent properties of the fibre and matrix materials in a composite are fixed, the greatest latitude in designing bulk composite properties is realized through tailoring of the interface (this is not strictly true, however, because processing conditions which lead to interface development also usually modify both the fibre properties as well as metallurgy of the matrix as discussed later). The development of an optimum interfacial bond between the fibre and the matrix is, therefore, of central importance. The nature and the quality of the interface (chemistry, morphology, strength and adhesion) are determined by factors both intrinsic to the fibre and matrix materials (chemistry, crystallography and defect content) as well as extrinsic to them (time, temperature, pressure, atmosphere and other fabrication-related variables). In the case of metal-matrix composites, a moderate amount of chemical interaction between the fibre and matrix improves wetting, assists liquid-phase fabrication of the composite and enhances the strength of the interface which in turn facilitates transfer of external stresses to the strengthening agent, i.e., the fibre. However, an excessive chemical reaction would degrade the fibre strength and defeat the very purpose for which the fibres were incorporated in the monolith. On the other hand, if toughening rather than strengthening is the objective, as in brittle matrix composites, then creation of a weak interface is desired so that crack deflection and frictional stresses during sliding of debonded fibres would permit realization of toughness. Thus, matrix interface and fibre properties must all be considered in composite design together with the fibre–matrix–interface interactions which usually modify the overall composite performance. This article reviews some basic aspects of evolution of interfaces in selected composites synthesized using the liquid-phase fabrication techniques.

Bonding at the fibre–matrix interface develops from physical or chemical interactions, interfacial frictional stresses, and thermal stresses due to mismatch between the coefficients of thermal expansion (CTEs) of fibre and matrix materials. In many metal-matrix systems, improvements in wetting and bonding can be achieved by a chemical reaction that yields as product phases chemical compounds (e.g., spinels or other oxides isostructural with spinel) which form strong bonds with both metals and ceramics. In contrast, in the case of brittle-matrix composites, recipes designed to improve the wetting at the fibre–matrix interface could induce too high a bond strength which will confer poor toughness on the composite. Thus a delicate balance between several conflicting requirements is usually necessary in order to tailor interfaces for a specific application with the aid of surface engineering and processing science.

Chemical interactions between the fibre and matrix manifest themselves in a variety of forms, e.g., interdiffusion and solute segregation, dissolution–precipitation, adsorption and reaction product formation. Chemical interactions often result in the formation of

intermediate non-equilibrium phases during evolution of interface to a more stable configuration (interfaces are thermodynamically unstable, and morphological and structural transformations continue well after fabrication). Besides chemical interactions between the fibre and the matrix, the thermoelastic compatibility between the fibre and the matrix must also be considered. A large CTE mismatch between the fibre and the matrix can give rise to large thermoelastic clamping stresses (compressive on the fibre when its expansion coefficient is smaller than that of the matrix) during cooling from the fabrication temperature. These stresses could give rise to interfacial cracking if the matrix cannot accommodate these stresses by plastic flow or dislocation generation. Intriguing new concepts which employ interface modification through compliant layers are being explored [1, 2] in advanced fibre-reinforced composites for high-temperature applications. The primary objective of these compliant layers is to reduce the CTE mismatch-induced thermal stresses and to improve the interface strength while providing adequate protection to the reinforcement against chemical degradation in reactive matrices. Finally, mechanical keying and interfacial friction could be caused by rough topography of the interfacial zone which arises either owing to growth-related surface flaws in the virgin fibre itself or owing to chemical-reaction-induced fibre surface reconstruction. The interfacial shear strength due to a purely frictional bond is, however, inferior to that due to chemical bonding.

The chemical interactions between the fibre and the matrix drastically alter the fibre properties and the metallurgy of the matrix. For example, the extent of fibre strength degradation due to chemical reactions is directly related to the amount of interfacial reaction [3–11]. Likewise, the consumption of valuable matrix solutes in interfacial reactions could impair the age-hardening response of the composite. The influence of interfacial reactions on fibre strength is established by correlating the strength of metal-coated fibres, or fibres extracted from the matrix of a composite material after suitable heat treatment, either with the thickness of the reaction zone [12] or with annealing conditions [13]. The propensity for and the extent of the fibre–matrix interaction depends upon the matrix chemistry, the fibre properties and the test conditions. From a materials development standpoint, understanding and controlling the interfacial phenomena in practical composite systems is a basic requirement for developing structurally viable metal-matrix composites.

2. Wettability

Wettability governs the fibre-matrix compatibility and is traditionally characterized in terms of an angle of contact that the liquid makes on the solid (Fig. 1). The well-known Young–Dupré equation [$\gamma_{1v}\cos\theta + \gamma_{1s} = \gamma_{sv}$] defines the equilibrium contact angle θ in terms of mechanical equilibrium of interfacial tensions γ_{1v}, γ_{1s} and γ_{sv} at the liquid–vapour, liquid–solid and solid–vapour boundaries, respectively. Other

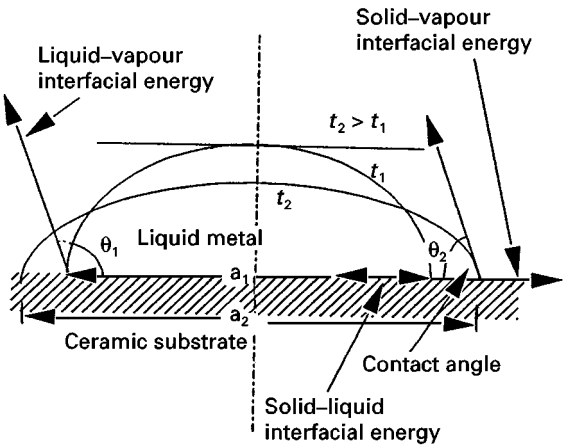

Figure 1 Diagram showing the concept of a wetting angle in terms of interfacial tensions at a three-phase junction.

measures of wettability are work of adhesion and wetting coefficients [14]. The concept of a work of adhesion is particularly useful in the study of composite interfaces, and is defined from $W_{ad} = \gamma_{1v}(1 + \cos\theta)$. A high work of adhesion indicates good wetting whereas a low work of adhesion indicates poor wetting. The problem of spreading wetting has been studied from both a fluid mechanics point of view as well as a surface physics point of view [15, 16].

In a strict thermodynamic sense, the Young–Dupré equation applies only to ideal surfaces, i.e., surfaces that are chemically and topologically homogeneous. Real surfaces, however, seldom conform to the concept of ideal surfaces. Chemical and structural inhomogeneities [17, 18] are the principal sources of non-ideality; these inhomogeneities give rise to thermodynamic (time-independent) hysteresis (e.g., due to surface roughness) and kinetic (time-dependent) hysteresis (e.g., due to chemical potential gradients). Furthermore, as the instantaneous value of contact angle depends upon the velocity of the contact line [14, 19–21], the dynamic angle is generally different from the static or equilibrium angle [22, 23]. Many commercial fibres contain growth-related surface flaws (e.g., surface asperities) which give rise to a microscopically "rough" surface. At large spreading velocities (i.e., at large capillary numbers $Ca = \mu U/\gamma_{1v}$, (where μ is the viscosity and U is the meniscus velocity), the liquid meniscus virtually "slips" over the asperities without penetrating the wedges between surface asperities. On the other hand, at low velocities, the wetting front is temporarily anchored to an asperity before breaking loose and moving quickly to the next anchor. Under these latter conditions, inertial forces become important in addition to viscous and surface forces. The wetting angles on completely wettable, topologically rough surfaces are related to equilibrium wetting angles by the Wenzel [24] equation ($\cos\phi = r\cos\theta$, where r is the ratio of the true wetted area to the apparent area, and α is an apparent contact angle). However, if roughness consists of sharp grooves, partial rather than complete wetting will result, and the Wenzel equation will not be valid. The surface roughness is characterized using a profilometer in which a stylus tip traces the surface profile

(wavelength and amplitude). This allows mathematical functions to simulate the surface roughness, e.g., a cosine profile with a Gaussian distribution of amplitudes [25]. Roughness may be important in other ways too; for example, the actual length of the contact line will increase because of roughness and, in the case of reactive fibre–metal systems, a larger surface area of contact will enhance the extent of chemical interaction.

The reinforcement surface is frequently modified by pre-treatments and coatings prior to composite fabrication; however, if the fibre surface transformation is incomplete, complex patterns of non-wetting and wetting regions would form on the fibre surface. Under these conditions, wetting hysteresis is observed owing to chemical or structural inhomogeneity [26–28]; hysteresis exists only if the scale of the inhomogeneity is such that the "stick–slip" motion of the liquid is not overcome by the amplitude of thermal wandering of the liquid meniscus (minute surface defects of nanometre size can distort and pin the contact line [27]). The wetting angles measured using the classical sessile drop technique depend upon the liquid volume in the droplet (drop size effect) [29]. Also, the mechanical equilibrium of a droplet resting on a flat solid surface can be violated if the normal component of the interfacial tension $\gamma_{1v} \sin \theta$ is large enough to cause deformation of the substrate [30–32]. While the Young–Dupré equation defines macroscopic wetting angles, in many systems, the macroscopic wetting front is spearheaded by a thin "foot" or a "precursor film". In such a case the macroscopic wetting angle is replaced by microscopic wetting angles which, in the general case, do not follow the Young–Dupré equation [33]. The precursor film is formed when the liquid has a finite non-zero curvature near its periphery owing to local molecular forces. In chemically reactive systems such as Cu–Sn, Fe–Sn, Cu–Zn, Fe–Cu and (Cu–Cr)–C couples [34, 35], reaction product phases form ahead of the wetting front by the process of surface diffusion and/or by evaporation–condensation and alter the interfacial equilibria. In spite of all such limitations and exclusions, the concept of wetting angles as defined by the Young–Dupré equation is useful in a wide variety of materials processes. The application of classical surface thermodynamics to kinetics of braze spreading and melt impregnation of sintered porous bodies [36–40] has led to considerable insights into these processes.

Wettability measurements on bulk solids may not be representative of wettability of solids in the form of fibres and particles and, as such, direct measurements (sessile-drop test) on compressed powders may not be reliable. In such cases, wettability is characterized by measurement of pressure for liquid displacement in powders beds, by liquid intrusion porosimetry or by dynamic measurements of rate of capillary penetration. In another method, called the "immersion" technique or the "dip-coverage" method, the fraction of area wetted is measured after the solid is withdrawn from the melt [41, 42]. The fraction area covered versus time plots are usually S shaped (sigmoidal) and are consistent with a time-dependent nucleation and growth mechanism of wetting [41, 42].

3. Prediction of interfacial energies

The wetting of ceramics by liquid metals is influenced by a number of variables such as heat of formation, stoichiometry, valence electron concentration in the ceramic phase, and the temperature, time, atmosphere, roughness and crystallography of the ceramic phase [43–53]. It is well known that the work of adhesion between a ceramic and a metal decreases with increasing heat of formation of carbides. The high heat of formation of stable carbides implies strong interatomic bonds and correspondingly weak interaction with metallic melts (poor wetting). Thus, highly ionic ceramics such as alumina are relatively difficult to wet since their electrons are tightly bound; the interfacial energy between alumina and metals increases roughly with increasing cohesive energy (melting point) of the metal. Metallic and covalent bonds are more similar in character and covalently bonded ceramics are more easily wetted by metals (and are more likely to react with metals) than highly ionic ceramics. High valence electron concentration generally implies lower stability of carbides and improved wettability between ceramics and metals. High temperatures and long contact times usually promote chemical-reaction-induced wettability. Gas adsorption on solids, impurity segregation, and surface defect structure all influence the interfacial energy of solids. Suboxide surfaces created by electron irradiation, ion bombardment or thermal decomposition are chemically reactive and display increased wetting by metals. Numerous studies have been carried out to measure and enhance the wetting of ceramics with metals [54–95], and the role of wetting and capillary phenomena in solidification processing of composites has been extensively reviewed [50, 53, 95–100].

The modelling and prediction of interfacial energies, work of adhesion and contact angles have been a focus of many studies [43, 96, 97, 101–106]. Earlier models [105, 106] considered wetting to be related to the oxygen affinity of metals, with the work of adhesion, W_{ad}, determined by the ionic and van der Waals bonding. These models, however, ignore chemical interactions and predict that W_{ad} should decrease with increasing temperature, but often the opposite behaviour is observed. The thermodynamic models based upon an equation-of-state relationship [107–109], which were originally developed for low-energy organic systems, have been applied with limited success to ceramic–metal couples [110–113]. Here, an equation of state of the form $\gamma_{1v} = f(\gamma_{sv}, \gamma_{1v})$ is formulated and is used in conjunction with Young–Dupré equation, and experimental measurements of γ_{lv} and θ, to determine the other interfacial energies. The relationship between work of adhesion and fracture energy (an experimentally accessible parameter) is also used [114, 115]; however, plastic deformation, coherency strains and interfacial roughness tend to yield values for the work of adhesion which are overestimates.

The interfacial segregation of surface active solutes is an important consideration in theoretical predictions of wetting behaviour. Segregation occurs when the impurity causes a decrease in the surface energy; the component with the lower surface energy

preferentially segregates at the interface in agreement with the Gibb adsorption equation. For example, in Al–Mg alloys, the surface tension of Mg is lower than that of Al at the latter's melting point, and surface segregation of Mg leads to breakdown of protective surface oxide film. Theoretical models for surface segregation of solutes employ the Gibbs adsorption equation, the Langmuir–McLean equation [53], and the Miedema model [116, 117]. As most of these models were developed for grain-boundary and surface segregation in solids, their application to interfacial segregation in ceramic–metal composites has been of limited use. Segregation is also affected by the interface structure, the lattice mismatch and the presence of misfit dislocations. The difficulty in analysing interfacial segregation is compounded in multicomponent alloys because the local flux of each component depends upon the composition gradient of all other components in the system. Finally, atomistic models of interfaces (cluster calculations, supercell models and the "jellium" model) have also been developed. While these models are theoretically interesting in understanding the physics of interfaces, at present they are of limited utility in designing interfaces in real composites where interfacial segregation, chemical reactions and relatively large lattice disregistries render theoretical predictions difficult.

4. Wettability and interfacial reactions in selected systems

Wetting and interfacial adhesion are promoted by dissociation of surface oxides, chemical dissolution and interfacial compound formation, and interfacial adsorption of surface active solutes without chemical reaction product formation [43, 44, 55, 56, 96, 115–128]. It is generally believed that the higher the reactivity in a system, the better is the wetting. However, a key factor in wetting is not just the intensity of the reaction but also the wetting properties of the resulting interface [101, 102]. In fact, wetting and reactivity may vary in opposite directions [101]. Thus, a criterion for selecting an alloying element to promote wetting is not just its reactivity with the solid but also its ability to form a wettable interphase at the interface.

4.1. Carbon–metal systems

4.1.1. Wettability

Carbon is a covalent high melting-point solid that is characterized by closed stable electron configuration and high-strength interatomic bonds. Considerable differences exist in the wetting of carbon by liquid metals [35, 65–68, 71]. Transition metals show strong adhesion to carbon, and the work of adhesion is large (typically 20–25 Kcal mol^{-1}) owing to chemical interactions. On the other hand, metals of the secondary subgroups-B in groups IV, V and VI of the periodic table (Cu, Ag, Au, Zn, Cd, In, Ge, Sn, Pb, Bi, Se, Te, etc.) show small chemical affinity for carbon and poorly wet it. In the absence of chemical interactions, weak physical dispersion forces dominate the wetting

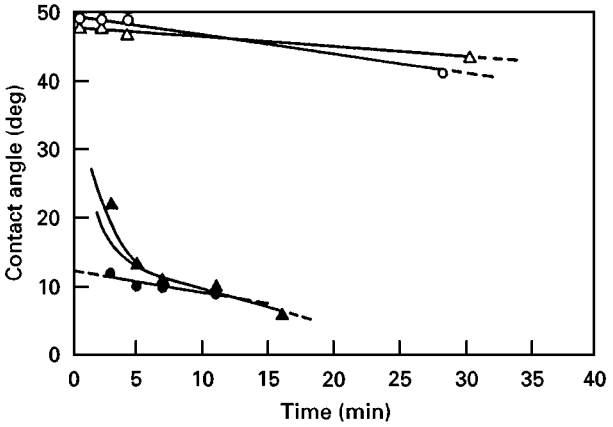

Figure 2 Variation in the wetting angle of Si on different carbon substrates as a function of time [62]. (○), vitreous carbon rod, cross-section; (△), vitreous carbon rod, longitudinal; (●), pyrolitic graphite, 0001 plane; (▲), pyrolitic graphite, 1000 plane.

behaviour; as a result, wetting is poor. Alloying elements improve or impair the wettability depending upon their surface activity. Thus, magnesium in Al improves the latter's wettability with carbon remarkably, and wetting angles in the range 20–55° are obtained at 1100 °C [65]. Similar improvements in wetting occur when Al is alloyed with Ta, Ti, Hf, Zr and Cr [35, 66, 67]. On the other hand, Be in Al tends to impair the wetting of C with Al by increasing the tenacity of the oxide film on molten Al [48, 129] which prevents establishment of true contact between the metal and carbon.

In the case of copper on graphite, alloying Cu with Cr, V, Hf, Zr, Co and Fe [35, 68–70] reduces the contact angle. In the Au–C system, the additions of nickel to gold modifies its interface with graphite by segregating at the interface and forming an adsorbed layer [130]. In the wettable C–Si system, a vigorous exothermic reaction takes place which is accompanied by a decrease in wetting angle to near-zero values (Fig. 2); the nature of carbon substrate (e.g., pyrolytic or amorphous) together with the atmosphere and temperature influence the wetting angles [62]. The wettability of carbon with metals is enhanced by heat treatment and surface coatings. Heat treatment raises the solids surface energy by causing desorption of adsorbed contaminants [95]. Surface modification by coating deposition enhances the wettability and/or creates a diffusion barrier to inhibit strength-limiting interfacial reactions. Metallic coatings on carbon and other reinforcements in Al [82, 95, 131–135], Pb–Sn and Zn [72], oxide coatings on C fibres in Mg [73, 74], ceramic overlays (C/SiC, C/TiC, C/TiN) on C fibres in Al [75], and fluoride (K_2ZrF_6) coatings on carbon fibres in Al [76, 129] are some common coating materials for carbon. In the C–Mg system, wetting is improved significantly by adding fine particles of Mg nitride to the matrix metal [77], by electrolytically depositing metal coatings on fibres [78], and by vapour-phase deposition of titanium and Ti–B compounds [79, 80] on fibres. Other techniques make use of modification of C fibre reactivity by alkali metal intercalation [81], and deposition of sol–gel-grown

homogeneous oxide films such as zirconia [83, 84]. In the sol–gel coating process, an ultrafine suspension of an appropriate alkoxide is gelled in the presence of the reinforcement. The viscous gel nucleates on the reinforcement surface to form a continuous adherent coating. During composite fabrication, however, the temperature and time of exposure must be carefully controlled to prevent rapid degradation of the coating. Chemical reactions of certain zirconia containing fibres (e.g., DuPont's PRD 166 fibres) with molten Al [136] and Ni–Al [137] alloys result in extensive reaction of zirconium oxide with Al.

4.1.2. Interfacial reactions

In the C–Al system, only one stable carbide Al_4Cl_3 forms; however, the reaction path leading to formation of Al_4C_3 could involve intermediate metastable phases. Because of its extreme affinity towards oxygen, liquid Al is covered by a thin (native) oxide film which reacts with carbon to form metastable aluminium oxycarbides. Carbon diffuses through this layer into the liquid which becomes supersaturated with respect to Al_4C_3 and this carbide is precipitated in the liquid ahead of the aluminium oxycarbide layer. Small additions of Ti to Al modify the reaction, yielding first a precipitation of small TiC particles (Fig. 3) which nucleate heterogeneously on already existing Al_4C_3 crystals. At higher Ti contents, Ti_2AlC and $TiAl_3$ phases precipitate from the liquid and react with Al_4C_3 to form titanium carbide. As a result, the Al_4C_3 phase dissolves and titanium carbides are precipitated by homogeneous nucleation in the liquid metal. During infiltration of graphite fibres by Al–Ti melts, a large number of TiC crystals form at the entrance region of the preform which reduce the permeability and impede the infiltration [138]. The reaction to form TiC also decreases the titanium content in the liquid and TiC formation further in the preform is inhibited. The reaction continues to the point where either the Ti content becomes sufficiently low to render Al_4C_3 more stable or until all the graphite is consumed. The formation of brittle and hygroscopic aluminium carbide leads to strength degradation in the C–Al composites.

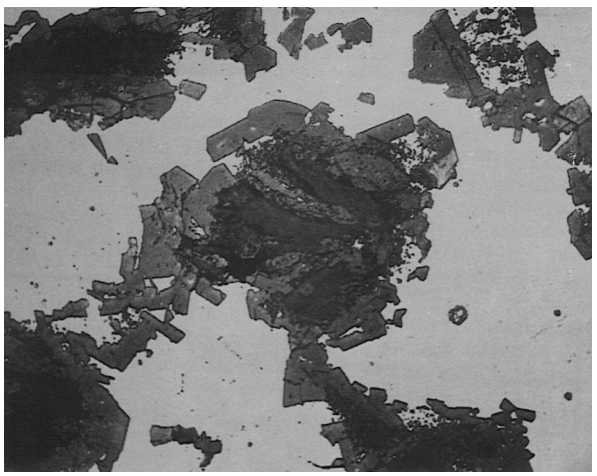

Figure 3 Photomicrograph showing extensive attack of carbon particles by an Al–Ti alloy [135].

In the C–Mg composites, no gross reaction products are usually detected, although magnesium carbide (MgC_2 and Mg_2C_3) formation is thermodynamically feasible [139]. On the other hand, when lithium is present in magnesium as an alloying element, C fibres react with the matrix, yielding the brittle carbide (Li_2C_2) which results in fibre cracking and strength loss [140, 141]. In graphite–copper composites, chromium is added to improve the wettability and facilitate infiltration owing to formation of a chromium carbide layer at the interface [142]. Differences in the crystal structure, stoichiometry and purity of carbon result in different levels of strength loss owing to chemical attack; for example, strength degradation is less in pitch-based C fibre than in polyacrylonitrile (PAN) based fibres when aluminium is used as a matrix material.

4.1.3. Control of interfacial reactions

The chemical degradation of carbon fibres in metal matrices can be reduced by controlling the process parameters and/or by suitable matrix alloying, e.g., by alloying Al with Si or Ti in graphite–(Al–Si) and graphite (Al–Ti) composites, respectively [143]. Reaction barrier coatings on carbon also inhibit strength-limiting interfacial reactions. Carbon and graphite fibres coated with silica, silicon carbide, titanium and boron are used in aluminium and magnesium matrices. The range of coatings on carbon includes metals (Cu, Ni, Ag, Cr, B, Mo, Si and Ta), borides (TiB_2, ZrB_2 and HfB_2), carbides (SiC, TiC and ZrC), oxides (ZrO_2), and nitrides (BN and TiN) [144–153]. Electroplating, electroless plating, chemical vapour deposition (CVD) physical vapour deposition (PVD), thermal decomposition, sputtering and melt immersion are common coating methods. Process control during coatings deposition is important because fibre damage due to coating deposition, and exothermic reactions between metal and coating material could degrade the fibre strength. Multilayer, multifunctional coatings are deposited to create wettable interphases, diffusion barriers and stress-absorbing compliant layers. Thus, PAN-based high-strength C fibres have been coated with various double layers consisting of a carbon underlayer and a ceramic overlayer such as C/TiC, C/TiN, C/SiC, followed by a final coating of a Ti–B mixture for compatibility with molten Al [154].

Titanium and boron are effective reaction barriers (and good wetting agents) in Al and Mg melts, but they are not air stable and undergo oxidation in air atmosphere with the passage of time, leading to degradation of fibre strength [149–151]. Oxide coatings such as silica on carbon dissolve in magnesium alloys together with the formation of Mg_2Si and MgO particles. Interfacial reactions suppress formation of certain alloy phases in the matrix because of the consumption of solutes in the reaction which upsets the bulk matrix concentration [155, 156]. The matrix metallurgy and its influence on post-fabrication heat treatment such as age hardening is then drastically altered.

Reinforcing light alloys such as Mg–Li and Al–Li with carbon fibres could yield high-specific-strength materials for structural applications. Because the Mg–Li–C system is thermodynamically unstable [140, 141], a pyrocarbon coating on the fibre is used to provide an effective barrier against lithium penetration into the C lattice. In the absence of a pyrocarbon coatings, Li atoms rapidly enter the graphite lattice at elevated temperatures and, after losing their electrons, they migrate as Li^+ ions through the carbon lattice by a thermally activated diffusion process. The most favourable routes for diffusion are the directions parallel to the basal (hexagonal) planes; diffusion of Li^+ ions across the basal planes is energetically unfavourable [157]. The pyrocarbon layers on carbon fibres are such that the basal planes of the coating are parallel to the *c* axis (long axis) of the underlying carbon fibre. The pyrocarbon layers from hydrocarbon precursors consist of benzene-type hexagons that form planar blocks oriented mainly parallel to the carbon fibre. Thus, relatively well-organized sheet texture of deposited pyrocarbon layers will limit lithium penetration and fibre embrittlement [158]. While the pyrocarbon layers protect the fibre, they tend to impair the fibre–metal wettability. The deposition of an outer SiC coating on the pyrocarbon layer restores the wettability.

4.2. Silicon carbide–metal systems

4.2.1. Wettability

Wetting angles in the SiC–metal systems have been measured as a function of alloying [86, 159–167], contact time [87, 164–167], temperature [87, 163, 165], atmosphere [96, 160] and SiC type (e.g., hot pressed, reaction bonded, single crystal [63]). In general, a transition from non-wetting to wetting occurs at high temperatures because of dissociation of surface oxides. Fig. 4 shows the reported temperature dependencies of contact angle in some SiC–metal systems. In the SiC–Al system under vacuum, a reaction of Al with the surface oxides produces gaseous suboxide Al_2O which erodes the oxides and establishes direct physical contact between SiC and metal. With a native surface oxide film (silica) on SiC, Al oxidation takes place and wetting is impaired owing to generation of alumina. As the reduction of silica by Al and formation of poorly wetting alumina could occur before attainment of equilibrium wetting, silica coatings may not be effective in promoting the wettability [103]; however, the influence of silica on wettability depends also upon the Mg content in the Al alloy (alloying Al with Mg improves SiC–Al wettability). In the Cu–SiC system, copper decomposes SiC and strongly dissolves into it [87]; the bonding between SiC and Cu is, however, inferior to bonding between Al and SiC. Pure metals such as Au, Ag or Sn do not wet SiC; however, a dramatic decrease in wetting angle is obtained by small additions of Ti or Si which promote wetting [168]. When the surface of silicon carbide is coated with metals such as copper and nickel, the threshold pressures for infiltration with Al is reduced and infiltration kinetics are enhanced because Cu and Ni wet Al and form solid solutions and/or intermetallic compounds [169, 170]. Similarly, titanium additions to Si in the SiC–Si system suppress the formation of silica and free carbon, and promote wetting and bonding [171].

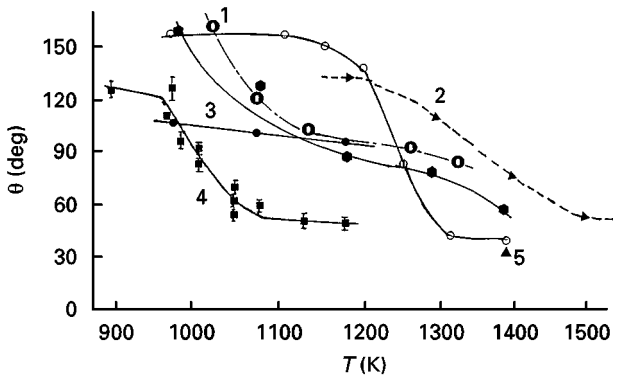

Figure 4 Wetting angle in the SiC–Al system as a function of temperature: curve 1, [160]; curve 2, [87]; curve 3, [167]; curve 4, [164]; curve 5 [43].

4.2.2. Interfacial reactions

The chemical stability of SiC in molten alloys, principally Al based, is important owing to the commercial potential of the SiC–Al composite material [158, 159, 172–200]. SiC reacts with Al to form brittle aluminium carbide (Fig. 5) which degrades the composite properties. The chemical reaction and the corresponding free-energy change are

$$3SiC(s) + 4Al(l) = Al_4C_3(s) + 3Si$$

$$G = 113\,888 - 12.05 \ln T + 8.91 \times 10^{-3} T^2 + 21.51T + 7.53 \times 10^4 T^{-1} + 3RT \ln a\mathrm{si}$$

The enrichment of the metal with silicon released from the carbide dissolution reaction lowers the liquidus temperature of the alloy and modifies its metallurgy. The rate of carbide dissolution reaction can be reduced by enrichment of the melt with free Si. In the case of Al–Si alloys, the equilibrium Si level increases from 8.4 wt % at 607 °C to 12.8 wt % at 827 °C [199]; so, if the Si content reaches these levels at the respective temperatures, the carbide dissolution reaction will become thermodynamically unfavourable. X-ray diffraction, wet chemical analysis, measurement of change in liquidus temperature, and various surface analytical techniques are used in conjunction with thermodynamic, kinetic and atomic models to study the reaction and bonding in the SiC–Al system. In the case of oxidized SiC, the oxide film thickness determines the reaction path. With a thin native oxide film on SiC, aluminosilicates and amorphous alumina from in Al-matrix composites; however, once SiO_2 is consumed, Al_4C_3 forms. With a thick (> 5 nm) oxide layer on SiC, only aluminosilicates and alumina form [201–203]. When Al is alloyed with both Si and Mg, the reaction kinetics are enhanced and product phases (alumina, Al_2SiO_5, $Al_6Si_2O_{13}$ or $MgAl_2O_4$) form. With oxidized silicon carbide, the surface oxide first reacts with Al(l) according to the exothermic reaction [204] $4Al(l) + 3SiO_2 \rightarrow Al_2O_3 +$

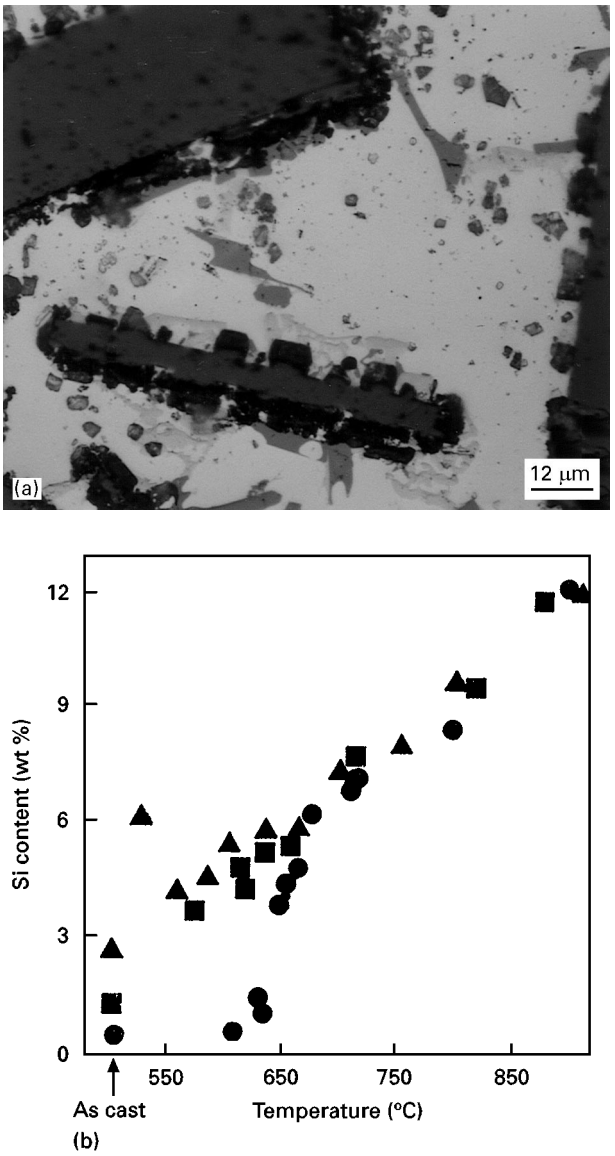

Figure 5 (a) Photomicrograph showing chemical attack of SiC by aluminium [169]. (b) Concentration of Si released in Al from an aluminium-carbide-forming reaction as a function of temperature [186] (●), unoxidized SiC; (■) oxidized (1000 °C for 18 h) SiC; (▲), oxidized (1000 °C for 100 h) SiC.

3Si. Once Al has reacted with the outer oxide layer on SiC to produce alumina, the direct reaction between Al and SiC proceeds at a rate similar to that found for unoxidized SiC. During initial stages, the kinetics of this reaction are very fast; in the later stages however, the rate of reaction is slow, the increment in the Si content of the matrix alloy being approximately proportional to time. In vacuum or under very low partial pressures of oxygen, the silicon dioxide surface film can breakdown according to the reaction $SiC(s) + 2SiO_2(s) \rightarrow 3SiO(g) + CO(g)$; as a result, the protective influence of silica on SiC may be lost even before contact with the liquid metal is established. Even with the silica films on SiC which impair the wettability with Al alloys [205] owing to formation of poorly wetting alumina, the presence of Mg in Al decreases the threshold pressure for infiltration [183]. However, the amount of Mg present in the alloy is of central importance. At low Mg contents, wetting improves by spinel ($MgAl_2O_4$) formation whereas, at high Mg contents, wetting is impaired owing to MgO formation. Extensive formation of the spinel during infiltration is consistent with the lowering of threshold pressures.

Conceivably, the rate of wetting promoting interfacial reactions should be rapid relative to the rate at which equilibrium wetting is attained. If, on the other hand, the kinetics of reactions which produce chemically and morphologically stable wetting-inhibiting compounds are rapid, then an intimate solid–liquid contact is not established. The reduction of silica by liquid Al to form aluminium oxide (a wetting-inhibiting compound) occurs very fast [205], and wetting does not improve because of rapid covering of SiC by the oxide. Thus, occurrence of an intense chemical reaction is not a sufficient condition for wetting enhancement [169–171, 206]; the interfacial reactions should yield product phases that form a low-energy fibre–matrix interface. Even when the test conditions preclude formation of low-energy interphases, the dissolution of the solid in the liquid and its reprecipitation on pre-existing solid could modify the surface [191; 199] such that good wetting and bonding take place without the formation of reaction products [207].

When a chemical reaction takes place between SiC and Al, the product carbide phase precipitates discontinuously and Si precipitates between the carbide crystals [158]. The aluminium carbide crystals first nucleate at preferred sites on SiC, SiC dissolution continues where SiC and Al are in direct contact, and finally dissolution of SiC occurs from areas separated by the interfacial reaction products [187, 208]. The interfacial product phase morphology (e.g., continuous film or extensive notch formation) controls the strength-limiting behaviour of the fibre. The differences in the SiC grain size could lead to different morphologies of the Al_4C_3 phase. In one study [91] on the chemical stability of SiC fibres and particulates in Al, Al_4C_3 crystals were observed to intrude between the individual columnar subgrains of the fibre; the faulted subgrains of the fibre were thus separated by regions of Al_4C_3. With particulate SiC, however, the grains, while faulted, were usually large and equiaxed, and the individual Al_4C_3 crystals were roughly of the same size as the parent SiC grains. Despite good interfacial bonding, fibre surface reconstruction due to interpenetrating regions of the two carbides would lead to localized stress concentration and limit the strength of the fibre [10, 209]. High dislocation densities at the interface also occur owing to large mismatch between CTEs [210, 211].

4.2.3. Influence of fibre characteristics on interfacial reaction

The carbide dissolution reaction has been observed in different structural varieties of SiC such as pressureless-sintered β-SiC [212], SiC fibres (Nicalon, Tyrrano and AVCO CVD fibres) [213], α- and β-SiC particles and platelets [158, 208], amorphous SiC film [214] and β-SiC whiskers [215]. The compositional and structural differences between different commercial

varieties of silicon carbide fibres affect their reaction with liquid metals. Thus, in cast Nicalon fibre–Al composites, Al_4C_3 forms at the interface whereas, in Tyranno fibre–Al composites, carbides do not form under identical test conditions [213]. Titanium introduced in the Tyranno fibre precursor decreases the reactivity of the fibre with Al by forming strong bonds between excess C and Ti, thus decreasing the affinity of excess C in the fibre to Al. Also Tyranno fibres have a lower C content (27.9 wt %) than Nicalon fibre (32.5 wt %). On the other hand, prolonged heat treatment degrades the Tyranno fibres more than the Nicalon fibres because the excess oxygen atoms in the Tyranno fibre (which exist as SiO_2 or as silicon oxycarbide, (Si_xO_y) react with pure Al to liberate Si which lowers the solidus and liquidus temperatures. A liquid phase, therefore, forms even at relatively low heat treatment temperatures as soon as a critical Si concentration is reached. The chemical attack of the fibre is then enhanced since the diffusion and growth kinetics are increased in the presence of a liquid phase. Textron's C-rich SiC filament (SCS fibres) and BP's Si-rich SiC fibre (called σ fibre) are two other popular SiC fibres for metal matrices. The SCS silicon carbide fibres exhibit good strength but poor wetting with Al; pre-oxidized filaments are used to improve the wetting but their strength is impaired on exposure to Al(l) at $T > 650\,^{\circ}C$. Addition of Ti, Mg or Ni to molten aluminium improves wetting of the SCS fibres; however, wetting is accompanied by reactions which reduce the fibre strength. In the case of BP's Si-rich σ fibres, a bilayer coating of TiC/C is effective in improving wetting and inhibiting reactions with Al [17]. While TiC coatings are stable in Al, direct deposition of TiC on SiC fibres reduces the fibre strength owing to thermal stresses generated at the fibre–coating interface during cooling from the deposition temperature which lead to coating fracture and spallation. An intermediate carbon layer between SiC and TiC acts as a stress-absorbing compliant layer which blunts cracks or diverts them from progressing into the fibre. The bilayer TiC/C coatings with fine grains are compatible with the SiC fibres and stable in Al to 950 °C [174]. However, in spite of the fact that no gross chemical reactions occur until these temperatures, diffusion of Al into SiC fibres and a slight diffusion of Si from the fibres into the Al matrix takes place; cracks form within the fibres in the regions where Al had diffused possibly owing to difference in the CTE of Al-rich zones within the fibres relative to the virgin fibre lattice. The presence of the C compliant layer is crucial; direct deposition of TiC without the C interlayer reduces the fibre strength from 3.50 to 1.68 GPa [174].

4.2.4. Control of interfacial reaction

Controlling the extent of brittle carbide formation in Al-coated SiC fibres by alloying Al with small amounts (1 at %) of Si allows retention of strength even after prolonged exposure to elevated temperatures [209]. On the other hand, fibres coated with unalloyed Al show a significant loss of strength. Fibre degradation can also be minimized by employing a variety of surface modifications [178, 216] such as surface oxidation by heat treatment, and formation of oxide coatings by the sol–gel or dry-mixing techniques. The basic approach followed in these techniques is to aid a quick reaction between the coating and melt to form a reaction barrier on the reinforcement. Oxide coatings such as SiO_2 and TiO_2 are active reaction barriers at relatively low-use temperatures because they quickly react with metals to form stable reaction products. The reaction of a SiO_2 coating on SiC with Al–Si–Mg alloys yields [178] a polycrystalline interfacial layer consisting mainly of Mg spinel crystals and Mg_2Si particles at low Mg concentrations, and fine MgO crystals at high Mg concentrations. The protective influence of a reaction barrier is influenced by its structure and porosity. As the SiO_2-to-spinel transformation is accompanied by a greater volumetric contraction than silica-to-MgO transformation, a porous interfacial layer of spinels forms which is permeable to Al. On the other hand, the transformation of silica to MgO in Al alloys with high Mg concentrations leads to a relatively small (about 14%) contraction, and hence only slightly oxidized particles can also provide an effective barrier to Al permeation and reaction with SiC.

The sol–gel technique uses a mixture of alkoxides dissolved in a solvent which deposits oxide coatings on the SiC. However, the sol–gel coatings of Al_2O_3 or MgO on SiC are not particularly effective reaction barriers but MgO coatings are relatively more effective than alumina. The dry-mixing technique uses mechanical mixing in a ball mill of the two types of particle (carbide and oxide) to produce agglomerated oxide particles adhering to the SiC. The technique has been used to coat SiC with oxide layers of TiO_2, Al_2O_3 or SiO_2; these coatings differ from one another in their effectiveness in protecting SiC in the melt. Thus, titanium oxide (TiO_2) coatings increase the incubation time for reaction and provide significant protection against attack by Al at 700 °C, but prolonged contact results in the dissolution of TiO_2 and SiC degradation [178]. These surface pre-treatments are cost effective compared with vapour-phase techniques (PVD and CVD) and are ideally suited to use in relatively inexpensive cast particulate composites.

The initial dissolution of SiC in metals is, to a first approximation, a zero-order reaction and the conversion increases linearly with time at a constant temperature [175, 192, 199]. As the growing interface reaches a particular thickness, the growth mechanism changes from dissolution to diffusion control, and the product carbide phase serves as a diffusion barrier, leading to characteristic parabolic growth kinetics. For example, in the SiC–Ti system, brittle reaction products such as TiC and Ti silicides form [12] by a diffusion mechanism with parabolic growth kinetics. The rate of these reactions can be significantly retarded by alloying Ti with Al, V and Nb [217–220]. Light alloys such as Mg–Li [140] and Al–Li [221], and the pure metal Li [222] react vigorously with silicon carbide. For example, Nicalon SiC fibres (SiC with 15% free C and 25% amorphous silica) and CVD monofilaments

absorb Li very rapidly during fabrication, causing grain-boundary embrittlement [141]. However, sputter-deposited yttria coatings are effective diffusion barriers which prevent Li ingress into the fibres. Also, single-crystal whiskers do not degrade in Mg–Li alloys even after prolonged contact. This is because of the relatively small negative free-energy change for the reaction of SiC with Mg–Li alloys, the slow reaction kinetics and the absence of inherent structural defects in whiskers.

4.3. Alumina–metal systems

4.3.1. Wettability

Sapphire, ruby and recrystallized alumina are not wetted by pure Al below about 1073 K [44, 91, 118, 223–233]. However, as wetting transitions are very sensitive to substrate roughness, oxygen partial pressures, crystal orientation and other factors, the temperature for wetting transition is seldom universal and well defined. In the case of recrystallized alumina, the wetting angle with Al attains a steady value at 1473 K [233] whereas on sapphire the droplet initially spreads and contracts repeatedly. In the sapphire–Al system, wetting angles are acute above 1223 K owing to complex oxygen-deficient interface structures which lower the surface tension. A gaseous suboxide (Al_2O) forms in vacuum above 1173 K which erodes the oxide film and reduces the wetting angle to less than 90° [227]. As the solubility of oxygen in Al is extremely low [230], different oxygen partial pressures in the atmosphere influence the oxide film thickness [229] and the wettability [225, 226].

Alloying additions have a pronounced effect on the wettability in the Al_2O_3–Al system. Alloying can either improve or impair the interfacial bond strength between alumina and metals [234–237]. For example, alloying Al with bismuth and selenium increases the interfacial shear strength with sapphire, whereas Cu and Zr reduce the interface strength [234]. Magnesium improves the wetting in the alumina–Al system (Fig. 6) even at relatively low temperatures [231], whereas Cu and Si are effective at relatively high temperatures (1173–1273 K). The interfacial segregation of Mg is common in ceramic–metal composites [95, 238, 239]. Both the oxygen-scavenging action of Mg, and its interfacial adsorption on and reaction with Al_2O_3 improve the wetting with Al (228, 240]. In a manner similar to Mg, cerium in Al alloys reduces the wetting angle on alumina ceramics, but the effect of cerium is less dramatic than that of magnesium. When more than one wettability-enhancing solutes are present in the alloy, their influence overlaps, e.g., in the case of aluminium alloys, when both magnesium and strontium are present, the wettability-enhancing tendency of strontium is masked by that of magnesium [241] which is a more potent wetting promoter. In Ni-based alloys, the wetting angle on alumina first reaches an equilibrium value but continues to decrease owing to dissolution of small amounts of impurities from alumina substrate, which results in large changes in the interfacial energy [242]. In Ag–In alloys in contact with zirconia and alumina, Ti additions improve wetting due to formation of TiO_2, TiO and Ti_2O [243]. In the case of intermetallic alloy Fe–40 wt % Al on polycrystalline alumina, B, Mg and Nb decreases the contact angle with increasing temperatures and time [244]. Oxide coatings such as MgO on alumina improve the latter's wettability with and dispersibility in stir-cast Al composites [94].

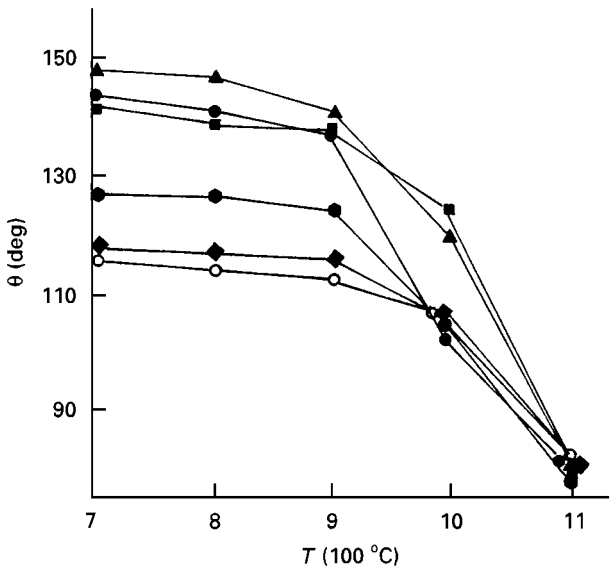

Figure 6 Influence of Mg content on the wetting angle of Al on alumina [231]. (▲), Al; (●) Al–1.33 wt % Mg; (■), Al–0.74 wt % Mg; (⬢), Al–3.9 wt % Mg; (◆), Al–3.9 wt % Mg; (○) Al–6 wt % Mg.

4.3.2. Interfacial reactions

A variety of alumina fibres are commercially available such as ICI's Saffil^{IM} (δ-Al_2O_3 with 3–4% SiO_2), Du Pont's fibre FP^{TM} (α-Al_2O_3 with silica coating) and PRD-166 (zirconia-stabilized alumina), Saphikon^{TM}s single-crystal sapphire and 3M's Nextel fibre. These fibres differ from one another in their chemistries, strengths, moduli and chemical stabilities. Thus, fibre FP of DuPont is a high-strength high modulus polycrystalline, 99% pure α-Al_2O_3 (grain size, 0.5 μm) fibre with a thin (5 nm) SiO_2 coating. Saphikon,^{TM}s single-crystal sapphire fibre is a high-strength (2.1–3.4 GPa at room temperature) high-modulus (414 GPa) fibre oriented along the *c* axis ⟨001⟩ of the hexagonal unit cell. Similarly, ICI's Saffil^{TM} is a polycrystalline δ–Al_2O_3 fibre with 3–4% SiO_2 added to stabilize the δ structure and to inhibit grain coarsening. Silica is also added as a thin colloidal coating to promote sintering of preform and to impart sufficient strength to resist compressive stresses that develop during squeeze casting. In these fibres, the silica coating does not change chemically (remains as silica or mullite) when the fibres contact molten Al or Al–Si alloys near the melting point of Al [245]. However, when Mg is present in the Al alloy, Mg ions are readily incorporated into the lattice of the fibre surface [246, 247], and reaction layers of spinel ($MgAl_2O_4$), MgO and fine polycrystalline α-alumina form at the interface. In the Al_2O_3–Al composites containing both Cu and Mg, the interfacial zones are composed of a duplex layer of copper spinel ($CuAl_2O_4$) and magnesium spinel

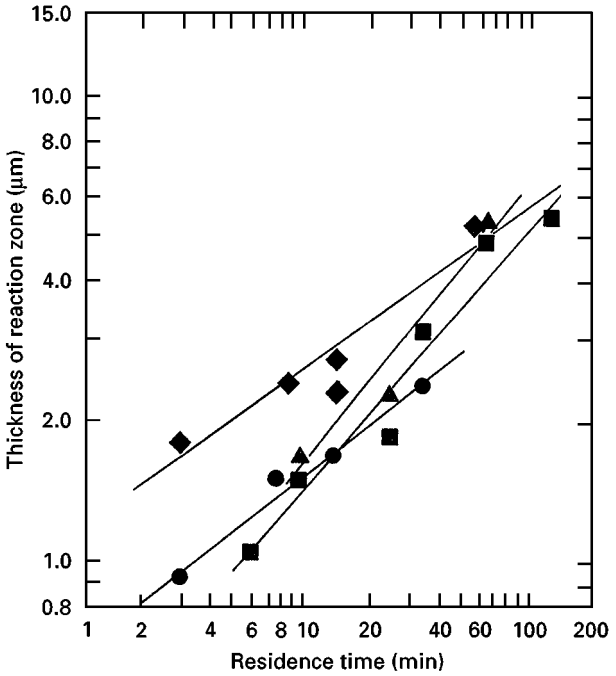

Figure 7 Reaction zone thickness in semisolid formed Al_2O_3–Al composites as a function of residence time of alumina in Al alloy [247]. (■), 2 wt % Mg (913 K); (▲), 4 wt % Mg (903 K) (●), 8 wt % Mg, (873 K); (◆), 4.5 wt % Cu and 2 wt % Mg (890 K).

($MgAl_2O_4$). The reaction pathways for interface development are sensitive to both alloying and processing conditions (Fig. 7). For example, copper spinel forms at the interface between fibre FP and Al–Cu alloys in composites fabricated using a compocasting (semisolid) technique [247], whereas no interfacial reaction product forms in pressure-cast composites [248] where interaction times are short. Silica as a fibre constituent or as a binder material in the preform reacts vigorously with the magnesium [249], and silicon released from the reaction combines with the residual Mg in the matrix to form Mg_2Si precipitates which assist precipitation hardening. Alumina fibres are chemically stable in Cu, but small additions of Ti to Cu cause a severe reaction with the alumina and formation of TiO_2. While wettability is improved by this reaction, the fibres experience loss of strength. The rate of this reaction is very sensitive to temperature and the reaction layer thickens with a diffusion-controlled mechanism [250].

4.3.3. Control of interfacial reaction

The deposition of reaction barriers and/or the formation of a stable reaction product during the early stages of fabrication will passivate the Al_2O_3 surface and inhibit further chemical attack. As reaction products usually form by nucleation and growth processes, a high nucleation rate may quickly generate a thin interfacial barrier layer which will isolate the reinforcement from attack by the melt. In Al–Mg alloys, where MgO and Mg spinels are the principal reaction products, a faceted and continuous layer of magnesium spinel ($MgAl_2O_4$) forms at high (7 wt %) Mg contents, whereas the reaction layer is patchy and discontinuous at lower Mg concentrations [251]. The thickness of the Mg spinel film on alumina decreases with increasing Mg content. A temperature-dependent incubation time characterizes the onset of reaction in this system; the incubation time drops discontinuously in the vicinity of 1000 K from about 2000 to 500 s.

Because a large driving force exists for the reaction of Mg with alumina, and the reaction kinetics are fast at elevated temperatures, an appreciable reaction zone could form even at short times [252], leading to fibre strength loss due to notch formation [247]. Fabrication conditions must, therefore, be carefully selected. The grain size of the product phase in the reaction zone is also important; for a fixed thickness of the reaction zone, larger MgO grain sizes yield inferior mechanical properties in the Al_2O_3–Al–Mg composites [253, 254]. An increase in the Al concentration in the alloy decreases the concentration gradient across the interface and inhibits the reaction. The interfacial reactions observed in fibre-reinforced composites also occur in discontinuously reinforced cast composites [187, 247, 255–258]; however, differences in the specific areas of the reinforcement results in different amounts of interfacial reactions.

In Mg–Li alloys reinforced with discontinuous δ-Al_2O_3 fibres (with the silica binder concentrated at free surface and grain boundaries), rapid penetration of lithium into fibre grain boundaries weakens the fibre [141, 257]. Lithium penetration into the fibres is accompanied by gradual transformation of the tetragonal δ–Al_2O_3 lattice into the cubic spinel $LiAl_5O_8$ where part of the Li^+ ions is substituted by Mg^{2+} ions. The fibres become brittle owing to formation of oxides (MgO and Li_2O), aluminates ($LiAlO_2$ and Li_5AlO_4) and spinels ($MgAl_2O_4$ and $LiAl_5O_8$). In Al–Li alloys, Li penetrates the fibres and reacts with alumina to form lithium aluminate ($LiAlO_2$) and lithium spinel ($Li_2O_5 \cdot Al_2O_3$) [259]; the microchemistry and the reaction zone thickness are extremely sensitive to processing conditions because of the high mobility of the lithium ions and the presence of short-circuit diffusion paths [260, 261]. High temperatures cause extensive fibre attack and grain coarsening. For example, fibre dissolution and grain coarsening take place in zirconia-stabilized alumina (PRD 166) fibres when they are infiltrated with a nickel aluminide matrix. Similarly, Al reacts with Du Pont's PRD 166 fibre, resulting in discrete particles of $ZrAl_3$ phase at the interface which grow rapidly into the matrix above the latter's melting point [263]. These undesirable interfacial reactions can be limited by employing short interaction times (infiltration times) in conjunction with low fibre pre-heat temperatures.

4.3.4. Alumina-reinforced high-temperature alloys

Fibre-reinforced intermetallics and superalloys are potential high-temperature materials for use in aircraft engine components. When these materials are fabricated using the solid-state powder-metallurgy (PM) processes [264], the contamination of the interface by organic binder residues and oxidation of metal powders prevent establishment of an

adequate interfacial bond. In contrast, melt-processed high-temperature composites such as Al_2O_3–NiAl and Al_2O_3–FeAl exhibit interface strength superior to that in hot-pressed composites [264–267]. Pressure infiltration casting is a popular liquid-phase fabrication technique for these materials. While chemical reactions, fibre dissolution, grain coarsening and enhanced dislocation density are observed in pressure-cast composites [268], liquid-phase techniques, in general, allow a better control of matrix and interface microstructures than solid-state techniques.

In cast sapphire-reinforced ordered intermetallic β-NiAl, an interfacial shear strength higher than that of the PM material is achieved without gross interdiffusion, in agreement with thermodynamic calculations [269]. Alloying NiAl with chromium, tungsten or ytterbium further improves the strength of the interfacial bond with sapphire [270, 271]. While tungsten is chemically inert and chromium is moderately reactive, the rare-earth element ytterbium (Yb) leads to a very severe attack of sapphire and a very high interfacial shear strength. Ytterbium oxide is thermodynamically more stable than aluminium oxide (the standard free energies of formation of Yb_2O_3 and Al_2O_3 are $-1727.5\,kJ\,mol^{-1}$ and $-1583.10\,kJ\,mol^{-1}$, respectively). However, in the sapphire–NiAl(Yb) system, a high interfacial shear strength is attained at the expense of fibre surface quality [270] which deteriorates owing to formation of Yb_2O_3 and $Y_3Al_5O_{12}$ at the interface (Fig. 8). In the powder-processed sapphire–NiA(Yb) composite, the dissolution of the fibre enriches the NiAl surrounding the fibre in oxygen. The diffusion of oxygen into the matrix and of Yb towards the fibres leads to the formation of a Yb_2O_3 layer around sapphire. Because of the oxygen enrichment of the original matrix powder used for hot pressing, Yb_2O_3 phase is also formed on the matrix grain boundaries (prior particle boundaries). The Yb_2O_3 phase located at grain boundaries in contact with the fibres reacts with alumina, leading to the formation of a spinel oxide ($Yb_3Al_5O_{12}$) which resides within the matrix grain boundaries adjacent to the fibre surface. Increasing the extent of reaction by remelting and controlled solidification of the powder-processed material leads to complete conversion of Yb_2O_3 to $Yb_3Al_5O_{12}$ (Fig. 8). A significant improvement in interface strength is achieved in melt-processed composites, but formation of interfacial shrinkage and microvoids impairs the interfacial bond strength.

In melt-grown sapphire–NiAl(Cr) composites [271] and sapphire–Ni couples [272, 273], the solid–liquid interface is preferentially enriched in fine chromium precipitates which appear well bonded to the solid (Fig. 9). The interfacial shear strength as well as the frictional sliding stress are higher in the sapphire–NiAl(Cr) composites than in the unalloyed sapphire–NiAl composites [271]. The Cr interlayers could potentially reduce the thermal stresses because of the lower CTE mismatch between sapphire and chromium compared with that between sapphire and NiAl. Controlled directional solidification of fibre-reinforced off-eutectic ternary Ni–Al–Cr alloys would also permit design of dual-phase matrix microstructures (e.g., cellular or dendritic interfaces with eutectic at the boundaries) which may have some toughening potential.

4.4. Other reinforcement–matrix combinations

Interfacial reactions, interfacial adhesion and fibre strength have been characterized in a large number of other composite systems such as B–Al [274], B–Ti [3, 218], TaC–Al [275], W–$NbSi_2$ [276], silica–Al [277–281], Si_3N_4–Fe [282], boron carbide–Al [283, 284], zircon–Al [285], glass–Al [286], zirconia–metal (Cu, Ni, Co) [287] and fibre-reinforced superalloys [288]. Most of these systems are chemically reactive. For example, in the SiO_2–Al system, redox reactions are thermodynamically possible and a multiphase interfacial layer develops at the interface; alloying elements such as Bi, Sb and Cu retard the reaction kinetics and increase the incubation time for the reaction [280], whereas Mg does the reverse. The incubation time is sensitive to the atmosphere [278–280, 289] and is drastically reduced in vacuum compared with air [278–280] because of the presence of an oxide film on liquid Al in air. Extensive chemical attack of silica by Al is noted in pressure-cast and stir-cast composites. Thus, in pressure-cast Al alloy 7075 matrix composites containing fused silica aerospheres [290], a reaction zone forms which thickens on artificial ageing, and Si preferentially nucleates on aerosphere surfaces. In stir-cast silica–(Al–Si–Mg) composites [291], reduction of silica by Al and Mg releases Si in the matrix which alters the matrix chemistry from hypoeutectic to hypereutectic compositions, as evidenced by an increase in the total Si content of the matrix and by the formation of silicon cuboids characteristic of primary silicon nucleation. Another silica-based oxide filler for metal matrices is flyash [292] which is a byproduct of coal-fired thermal power plants. The principal chemical constituents of flyash are mullite ($3Al_2O_3 \cdot 2SiO_2$), quartz (SiO_2), magnetite–ferrite (Fe_3O_4–MgO), heamatite (Fe_2O_3) and anhydrite ($CaSO_4$). When flyash is infiltrated with aluminium at relatively low temperatures and/or short infiltration times, its reaction with Al is limited; however, at high temperatures and/or longer contact times, extensive chemical attack of flyash is noted [292].

Potassium titanate and aluminium borate whiskers [293, 294] are cost competitive with SiC, traditionally regarded as the best whisker reinforcements for metal matrices. In Al–Mg composites, both these types of whisker undergo a moderate chemical reaction which produces β-Al_2O_3 particles and magnesium spinels; with borate whiskers, specific crystallographic orientation relationships of β-Al_2O_3 yield a very strong interfacial bond. The geometrical features of these whiskers affect the interfacial reaction. For example, there is little reaction on the plane of the whiskers but some reaction is seen at the whisker ends; the uneven surfaces and corners of whiskers react more vigorously than plane surface. In the case of *in-situ* composites such as TiC–Al, where the reinforcement is produced within the matrix via a chemical reaction,

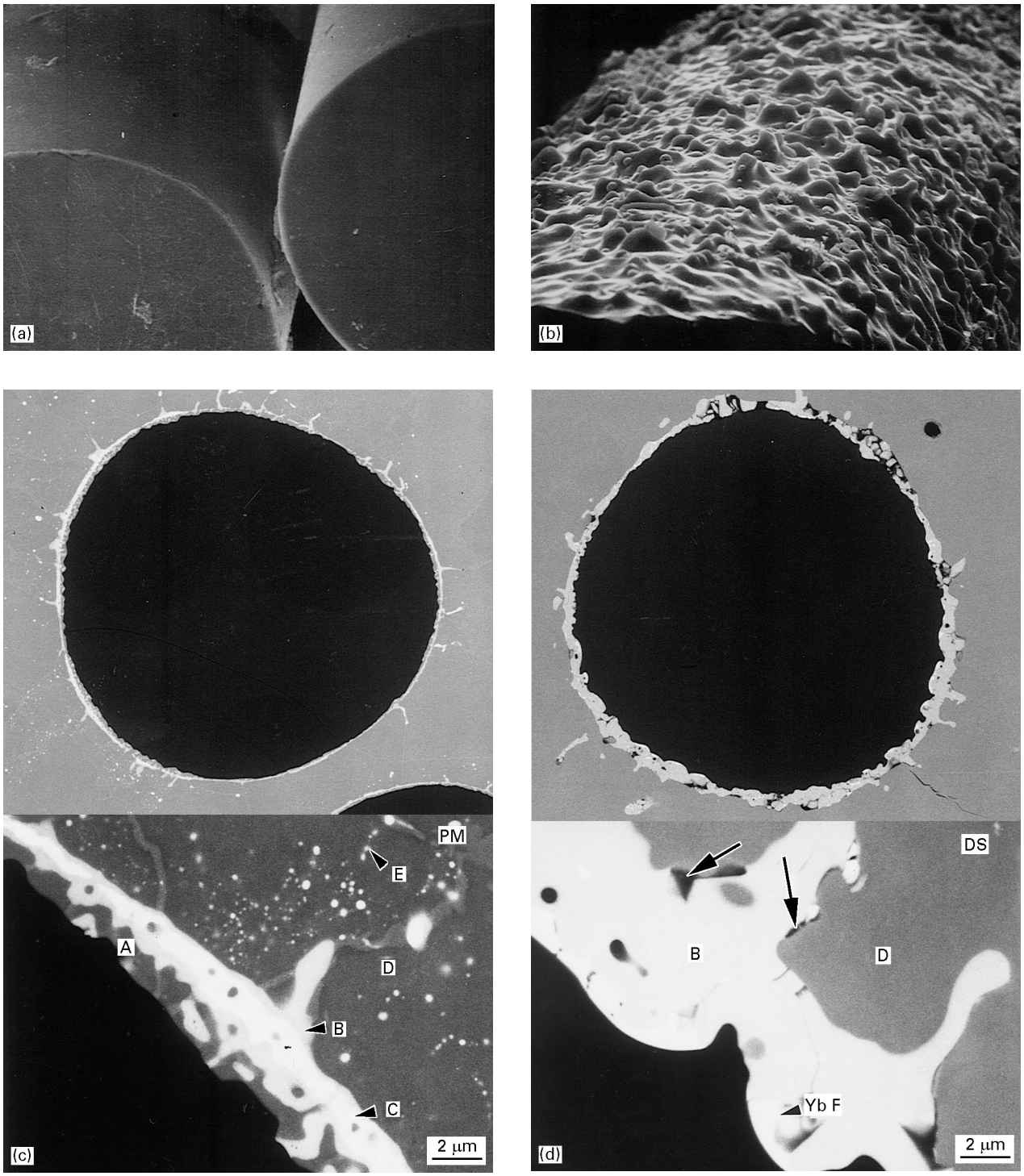

Figure 8 Photomicrographs showing (a) as-received sapphire fibre (b) fibre extracted from a sapphire–NiAl(Yb) composite showing extensive fibre surface reconstruction due to chemical attack, (c) interfacial reaction zone in a powder-processed sapphire–NiAl(Yb) composite and (d) interfacial reaction zone in a directional solidified sapphire–NiAl(Yb) powder-processed feedstock material [270]. In (c) and (d), A is O-rich NiAl, B is Yb_2O_3, C is $Yb_3Al_5O_{12}$, D is NiAl and E is YbF.

the interfaces are atomically clean and the interfacial bonding strong. For example, in the TiC–Al *in-situ* composites prepared by a melting and casting technique, the TiC particles show densely packed {1 1 1} planes parallel to the interface and a strong chemical bonding with Al [295].

5. Nature of interfacial reactions

The chemical dissolution of a reinforcement in the liquid matrix during composite fabrication occurs via heat, mass and momentum transport. Preform infiltration is a popular method for fabricating composite materials. Liquid metal flow during preform infiltration is usually laminar (Reynold's numbers, $Re < 10$). During chemical dissolution of a solid under laminar flow conditions, two types of boundary layer develop: a diffusion layer and a hydrodynamic boundary layer. The mass transport processes (diffusion and convection) can be modelled using appropriate theoretical relationships [296, 297]; diffusion will be the dominant mechanism of mass transport at small Peclet

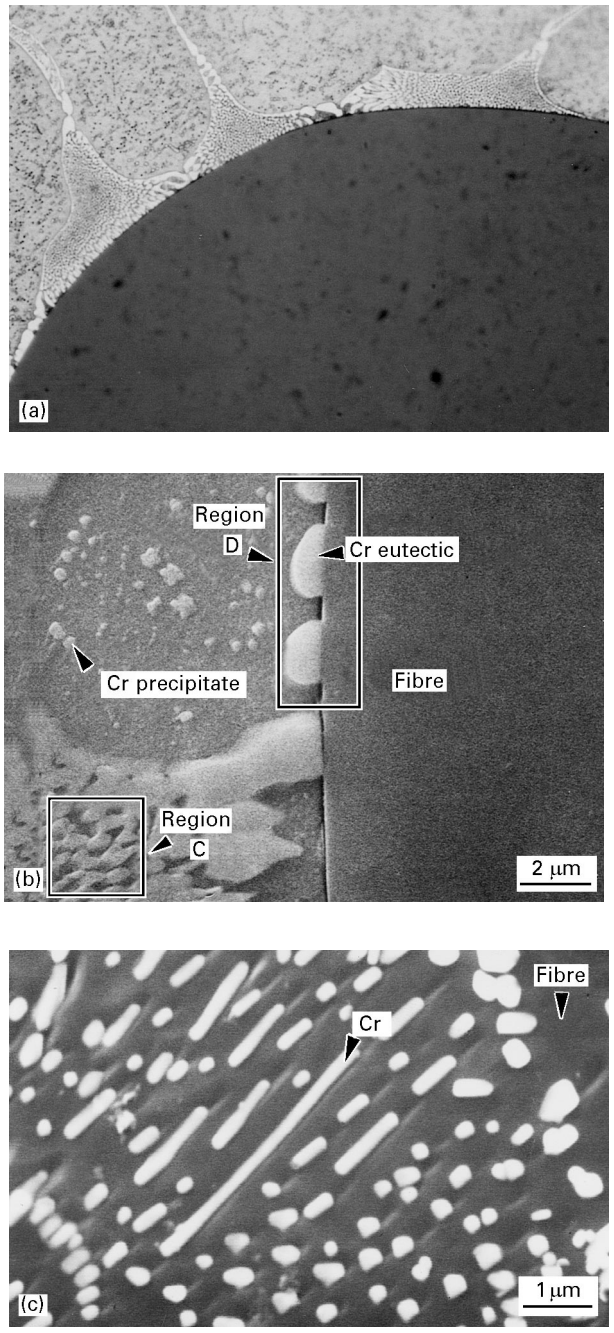

Figure 9 Interface region in a directional solidified sapphire–NiAl(Cr) composite showing. (a) preferential segregation of chromium at the interface, (b) good interfacial bonding between chromium and sapphire and (c) surface appearance of an extracted sapphire fibre showing chromium particles adhering to the fibre together with fibre pitting from chemical attack [271].

numbers Pe $\ll 1$ (Pe $= DV/R$, where D is the diffusion coefficient, V is the fluid velocity and R is the particle radius). At small Re, the reaction kinetics are parabolic in time ($X = kt^{1/2}$, where X is the thickness of the interphase and t is time) consistent with a diffusion mechanism. While diffusion controls interphase growth in many composities of practical importance such as B–Ti, C–Ni and SiC–Ti [298–301], interface reactions could become rate controlling in some systems (e.g., SiC–NiAl [302]). Non-planarity of the reaction interface and formation of intermediate metastable phases lead to a departure from a simple parabolic behaviour. Even when the test conditions preclude growth of reaction products, interdiffusion could generate solute gradients at the interface, resulting in interfacial segregation without compound formation.

The chemical reactivity of the fibre with the matrix forms a basis for classifying metal-matrix composites into three separate classes [298]: class I, reinforcement and the matrix are mutually non-reactive and insoluble, Class II, reinforcement and the matrix are mutually non-reactive but soluble; class III, reinforcement and the matrix are reactive and form at least one new compound at the interface and may also exhibit mutual solubility. Class I interfaces are seldom found in real composites of practical interest but serve as useful models to understand more complex interfaces. Most metal-matrix composites of engineering interest display class II and class III behaviours in which the complexity of the interface is compounded owing to non-planarity of the interface, crystal defects, chemical inhomogeneity, impurity segregation, formation of reaction products, and interdiffusion via surfaces, grain boundaries and other short-circuit paths unique to composites (e.g., network of touching fibres and platelets [303]). Thus, even with known thermodynamic and diffusion data, a first-principles-based prediction of interface evolution in class II and class III systems is complicated by a myriad of structure- and defect-related factors [304]. Local details of the interfacial microstructure influence the mechanical properties of composites, e.g., stress concentrations and crack deflection paths are dominated by interfacial topography. Because of such complexities, semiempirical models of interphase evolution are popular in engineering practice. The simplest approach in modelling reaction kinetics is to quantify the extent of reaction at any time, t, and to relate it through quantitative models to the time and temperature parameters. In a simple binary alloy with a reactive solute, the extent $\alpha(t)$, of reaction can be defined as [187] $\alpha(t) = [w_0 - w(t)/[w_0 - w_e]$, where w_0 is the initial solute content at $t = 0$, $w(t)$ is the solute content at any time $t > 0$, and w_e is the equilibrium solute content at that temperature. The extent $\alpha(t)$, of reaction can be related to the rate processes involved through semiempirical relationships. In the Al_2O_3–(Al–Mg) composites, a logarithmic variation in the amount of transformation product (Mg spinel) and Mg concentration with reaction time is observed. A temperature-dependent incubation time characterizes the reaction; the incubation time is about 2000 s at $T < 1000$ K but drops below 500 s at $T > 1000$ K. A number of possible mechanisms may be operative in the reaction, and the identification of the rate-controlling step(s) is not a trivial task. The value of activation energy for reaction gives some indication of the underlying reaction mechanisms.

The product phases in many systems such as Al_2O_3–Ni, Al_2O_3–Cu and Al_2O_3–Ti [304] are structurally and morphologically unstable. Furthermore, interfacial zones could exhibit over an order of magnitude variation in the grain size [305]. For example, in a study on melt-infiltrated fibre FP/ZE 41–Mg matrix composites, the reaction zone at the interface was on

average 100 nm wide [205] and comprised grains (primarily MgO) varying in size from less than 10 nm at the reaction zone–fibre interface to over 100 nm at the matrix–reaction zone interface. Preferential grain coarsening of MgO at the reaction zone–matrix interface together with the flow channel closure that stopped metal "seepage" towards the fibre surface during infiltration caused grain size variations within the interfacial region. Compositional inhomogeneity could also arise from preferential segregation of secondary phases at the interface (e.g., the two phases in a eutectic-type structure that precipitate on the reinforcement). These interfacial inhomogenieties lead to variations in the composite's response to heat treatment and mechanical stresses. For example, the interface strength in Al_2O_3–Mg composite decreases with decreasing reaction zone thickness and the off-axis strength of the composite decreases with decreasing size of MgO grains at the interface [254]. On the other hand, in model composite systems with controlled interfaces (e.g., Ti-coated C–Mg composites [306]), reliable predictions of bulk mechanical properties can be made using simple micromechanical models.

A common approach to limit fibre degradation in reactive matrices is the use of barrier coatings [307]. The diffusion barrier coatings must be compatible with both the matrix and the fibre; however, a lack of thermodynamic and reaction kinetic data often limits a premeditated design of coating systems for specific applications. The diffusion barrier coatings could be very elaborate, multilayered and multifunctional and could introduce additional interfaces that must assist in load transfer from the matrix to the reinforcement. The physical, chemical and mechanical stability of barrier coatings at use temperatures is important; protective influence of the coating will be lost if it transforms into an unstable or metastable product phase or loses its physical and mechanical integrity owing to thermal stresses. Mechanical breakdown of diffusion barriers often shows an incubation-type behaviour [8], i.e., visible signs of damage occur after a finite period of time has elapsed. Once the mechanical integrity of the reaction barrier is lost owing to breakdown of the barrier, chemical attack of the fibre produces undesirable reaction products. Thus, a thorough knowledge of reaction kinetics, phase equilibria, diffusion kinetics in complex multicomponent systems, and the micromechanical behaviour of product phase are needed for judicious selection of interfacial coatings.

The diffusional interactions across an interface are affected by interfacial stresses (e.g., stresses due to CTE mismatch and phase transitions); these stresses can adversely affect the microstructural stability during processing or subsequent service. If a large mismatch exists between the CTEs of the fibre and matrix materials, and/or temperatures excursions are large, appreciable thermal stresses could be generated. If these stresses are not accommodated by dislocation generation and matrix plasticity, failure will probably take place. In some systems (e.g., TiB–NiAl [172]), stresses are relaxed by the diffusion of large solute atoms in the interfacial region; this can occur because the matrix is under hydrostatic tension, and the oversized atoms can reduce the stresses.

6. Reaction mechanisms in selected systems

6.1. Carbon–metal systems

In the chemical reaction of carbon with molten Al to form aluminium carbide, carbon atoms first dissociate from solid's surface, diffuse through the interface interphases such as oxides and previously formed carbide and finally react with metallic Al to yield Al_4C_3. In the initial stages of the reaction, oxygen is chemisorbed on an active surface site, followed by electron transfer from graphite to the C–O pair, and the desorption of the pair as CO [308, 309]. The transferred electron strengthens the C–O pair bond while weakening the bond between surface C atom and the underlying graphite; this weakening permits the dissociation of surface C atoms and their diffusion across interface interphases. The aluminium carbide crystals nucleate heterogeneously on carbon and grow anisotropically as lath-like particles into the Al matrix by a ledge mechanism [310]. Later, during their coalescence, the carbide platelets grow into the fibres and the tensile strength decreases because of the random notches that form by growing Al_4C_3 platelets into the fibres. The addition of titanium diboride and boron or phosphorus compounds inhibits formation of Al_4C_3 [308].

In the C–Si system, the reaction between C and Si to form SiC is highly exothermic, and a dissolution–precipitation process appears to be operative. The reaction kinetics could be either diffusion controlled [311, 312] or interface controlled [313]. In the dissolution–reprecipitation process, the pre-existing SiC grains act as seeds for nucleation of new crystals [314]. There is an initial incubation for the reaction followed by a region of rapid growth that is roughly linear in time; this is followed by a progressive slowing of the rate as the reaction nears completion. While no gross reaction products form during incubation, a thin polycrystalline film forms which quickly spalls owing to its volume misfit relative to the underlying carbon [315]. During the rapid growth stage, larger faceted β-SiC crystals form adjacent to the SiC fibres whereas, within the fibres, fine SiC particulates form. The mechanism then becomes one of solution–reprecipitation, with the very fine SiC grains within the fibres serving as the source and the large faceted crystals serving as the sink. Dislocations form in large faceted grains but not in fine source SiC grains of the fibre; as a result, these fine grains do not self-coarsen. Reactive infiltration of porous carbon preforms by Si and Si–Mo alloys is used to form SiC–Si–C composites. The reactive infiltration of porous carbon is very rapid and proceeds to completion in a few seconds for preforms of the size of a few centimetres [315, 316]. As the amount of liquid phase diminishes very rapidly during reaction, the microstructural scale of the carbon preform must be both uniform and fine to avoid unreacted carbon. This can be accomplished by exercising control on process parameters during pyrolysis of

polymer precursors that are used in preparing the porous carbon preforms.

In the C–Cu system, chromium is usually added to improve the wettability and interfacial bonding. Here the diffusion of Cr out of liquid Cu and of carbon through the chromium carbide reaction layer control the growth rate [142]. Growth kinetics are parabolic in time. Initially, diffusion of Cr controls the reaction, and later, diffusion of C through the Cr_3C_2 layer controls the growth rate. The actual thickness of the Cr_3C_2 layer is strongly influenced by the geometry and specific surface area of the nucleating substrate [142].

6.2. Silicon carbide-metal systems

The chemical interaction of SiC with Al could proceed via penetration of Al into SiC and diffusion of Al into SiC [194]. Silicon carbide can dissolve into liquid Al at low temperatures without the formation of a chemical reaction product. The dissolved SiC is reprecipitated, and in the process some Al may be entrapped in between SiC crystals, leading to formation of channels of Al in the SiC. The dissolution and reprecipitation of SiC without Al_4C_3 formation is possible as long as Si is able to dissolve in the matrix while still providing a barrier to the formation of Al_4C_3, allowing the reprecipitation of SiC onto parent SiC. Penetration is also enhanced if stresses are present in the SiC; these stresses lead to formation of high-energy sites along the interface which aid the process of dissolution. In regions where the solid phase is stressed, dissolution takes place and, in regions that are stress free, the solid phase is reprecipitated. The coherency stresses generated during the diffusion process will cause the interface to attain a serrated shape. In the mechanism involving diffusion of Al into SiC, the actual diffusion of Al occurs by replacing the empty Si lattice sites generated by the dissolution of Si in the liquid metal. Aluminium is able to diffuse into SiC when the SiC is heavily damaged or when Si vacancies are available because of the presence of surface oxides. As Si dissolves in the matrix, a similar amount of Al is able to replace the missing Si atoms in the SiC lattice; this implies that Al can substitute for Si in the lattice as long as Si is able to dissolve in the liquid matrix. As a result, interdiffusion may occur without compound formation. On the other hand, when the test conditions lead to aluminium carbide formation at low temperatures (660 °C), a very small percentage of SiC particles react; so it is possible to miss the reaction by X-ray studies. Also, in commercial multicomponent Al alloys, several interfacial layers could form which obstruct the diffusion of Al into SiC. Under these conditions (especially if the interphase is porous), Al penetration rather than diffusion would be the dominant mode of chemical interaction.

The distribution of the Al_4C_3 that forms from the reaction is not uniform over all faces of SiC; flat and smooth surfaces are less favourable sites for carbide formation than rough surfaces. Single-crystal SiC whiskers grown along the face-centred cubic fcc $\langle 111 \rangle$ direction show significantly less reactivity than SiC particulates with irregular surface topography, although the nominal surface area of whiskers may be significantly larger than that of particulates [191]. In the case of single-crystal SiC, both Si (0001) face and the randomly oriented faces dissolve at a fast rate in molten Al, and aluminium carbide crystals nucleate onto the SiC surface with their c axis oriented parallel to the c axis of the SiC. Lateral extension of these crystallites results in the formation of a continuous layer of Al_4C_3 crystals that protects the substrate from further reaction. Passivation takes place sooner at the Si face than at randomly oriented faces of SiC. The C (0001) face dissolves at a much slower rate in Al than any other face but, as Al_4C_3 crystals do not nucleate onto this face, passivation never occurs. Consequently, after prolonged contact with Al and/or extensively high temperatures, the C face appears more damaged than any other face.

From the standpoint of atomic mismatch and lattice discontinuity at the interface, different crystallographic orientations are possible at the SiC–Al interface [172, 317]. When intermediate oxide films and Al_4C_3 are absent, interfacial energies and bond strength can be estimated from basic crystallographic parameters. The adhesion energy of the interface can be obtained from the energy of the SiC–Al atomic clusters. The minimization of cluster energy yields equilibrium separation between adjacent layers at the interface, as well as its adhesion energy. The energy necessary to create an interface is given by [317]

$$\Delta E = (E_{\mathrm{Al}} + E_{\mathrm{SiC}}) - E$$

where E_{Al} and E_{SiC} are the total energies of the Al and SiC clusters, respectively, and E is the total energy of the SiC–Al composite. This is calculated by varying the distance between cleaved surfaces of Al and SiC and the energy E corresponds to the minimum in this energy profile. The theoretical results based on the energy minimization approach suggest that bonding between Al and Si is slightly stronger than that between C and Al layer. The lattice mismatch and coherency strain considerations also suggest that interface between the (0001) plane of α-SiC should be parallel to the (111) plane of Al. However, high-resolution electron microscopy shows that (112) planes of Al bond to the basal planes of SiC [172]. This is because, in order to reduce the interfacial strain energy, the matrix planes would rotate to adopt an orientation that presents a more open structure (e.g., Al (112) planes) to the SiC basal plane.

7. Interfacial reactions, fibre strength and interface strength

Models which combine the theory of reaction kinetics and micromechanical behaviour of interfaces allow prediction of fibre strength as a function either of reaction zone thickness or of temperature and time of exposure. In the early stages of reaction, the defects caused by the interfacial reactions are less important than the inherent defects of the fibre, and the fibre strength remains at its original value. With increasing

reaction zone thickness, the effects of fibre surface reconstruction and notch formation become important in limiting the fibre strength. The reaction zone is brittle and fractures on loading at small strains. If the notch resulting in fracture forms at a stress, σ_{hf}, and extends into the fibre at a stress σ_{he}; then, if $\sigma_{hf} < \sigma_{he}$, the notch forms first and then extends into the fibre when the stress level reaches σ_{he}. If, however, $\sigma_{hf} > \sigma_{he}$, as soon as a notch forms it propagates catastrophically through the fibre. These stresses could be calculated from a knowledge of the tensile specimen dimensions, the Weibull strength distribution parameters, the fracture toughness of the fibre, the activation energy, and the elastic moduli of the fibre and the reaction products [5, 6, 13]. Phenomenologically, the tensile strength of fibres extracted from composites usually follows Weibull distribution according to which the probability of fibre failure; $F(\sigma)$ is given by $F(\sigma) = 1 - \exp(\alpha\sigma^{\beta})$, where β is the Weibull modulus and α is a scale parameter. The probability of fibre failure is related to sample population, N, by $F(\sigma) = i/N + 1$, where i is the ith fibre when the fibre strength data are arranged in an ascending order. Thus, the fibre strength follows the Weibull distribution if a plot of $\ln\{\ln [(N + 1)/(N + 1 - i)]\}$, versus $\ln \sigma$ is linear. Fig. 10 shows Weibull plots for the strength of alumina fibres extracted from selected pressure-cast Ni-based superalloys and intermetallics [318]. The fibres in these composites suffered strength loss of about 60–68% relative to the as-received fibres ($\sigma = 2.8$ GPa). Reactive solutes such as Cr, Ti and Zr in the matrix alloy chemically attack the alumina during fabrication, resulting in the formation of surface notches whose dimensions exceed the critical Griffith flaw size of as-received alumina (approximately 0.18 μm [11]). Similarly, strength degradation of about 45–60% is observed in powder-processed alumina-fibre-reinforced Fe–Cr–Al–Y, Fe–Cr–Al, FeAl, NiAl and Ni_3Al [11]. In spite of a somewhat greater strength loss in cast composites compared with powder-processed composites, a greater flexibility in designing the interface and matrix structures (e.g., tough dual-phase structures by controlled directional solidification) could make liquid-phase fabrication methods competitive with solid-state methods. A judicious control of reactive solutes in the matrix, use of reaction barriers, and control of processing conditions (temperature and time of exposure) will probably promote wetting and interfacial bonding while minimizing strength-limiting interfacial reactions.

The interfacial shear strength determines the stress transfer characteristics of the interface. Fibre push-out, pull-out, fragmentation tests, and fracture energy and laser spallation tests have been used [319–322] to make measurements of interface strength in fibre-reinforced composites. The fibre push-out test is a popular method for characterizing the interface strength in fibre-reinforced metal- and ceramic-matrix composites. The test measures the stress required to debond and slide a single fibre through thin wafers of the composite material. Typical stress–displacement profiles for the sapphire–NiAl intermetallic-matrix

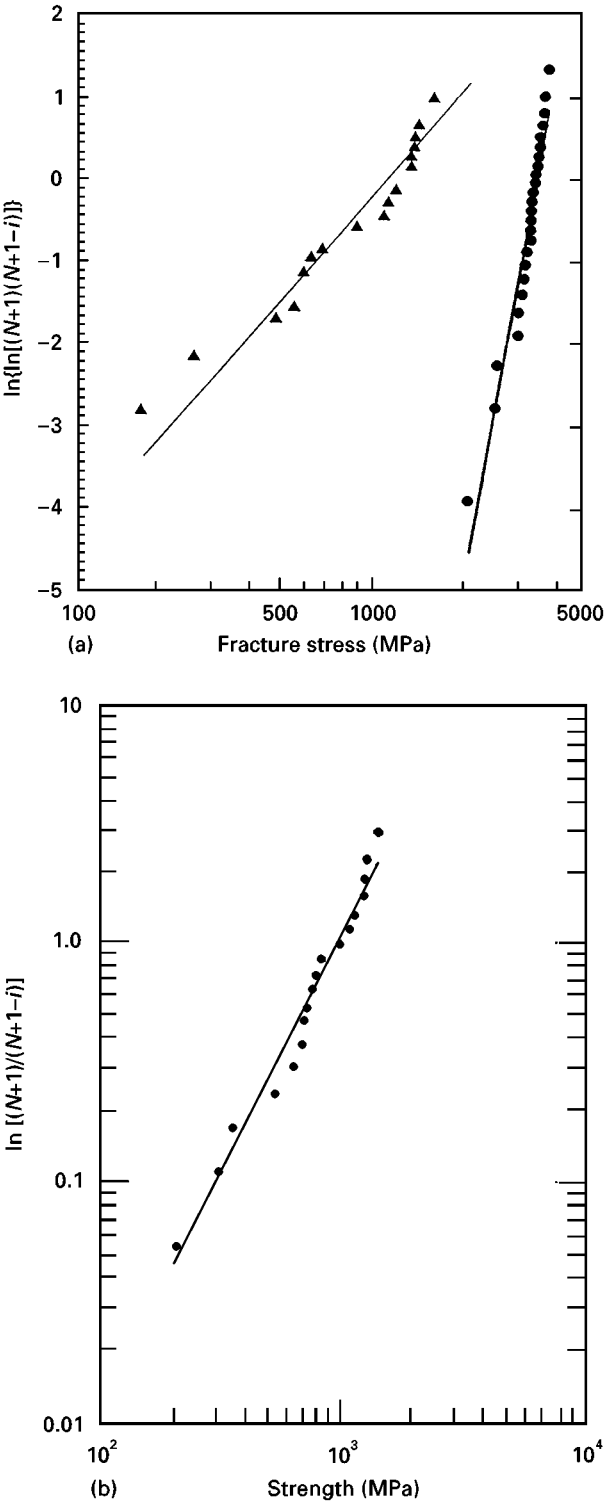

Figure 10 Weibull distribution of tensile strength of sapphire fibres under different conditions: (a) as-received fibre, [6] (●) and fibre extracted from a pressure-cast sapphire–Ni-based superalloy (Hastalloy) composite, (▲) [318]; (b) fibre extracted from a pressure-cast sapphire-Ni_3Al(Ti) composite [262].

composite wafers of different thickness are shown in Fig. 11 together with debonded interfaces in sapphire-reinforced NiAl(W), NiAl(Cr) and NiAl(Yb) alloys. The interfacial shear strength parameters for some sapphire–NiAl intermetallic-matrix composites are shown in Table I. Both the composite fabrication technique and the alloying influence the interfacial shear strength. The test methodology also influences the test results (e.g., thermal clamping and bending

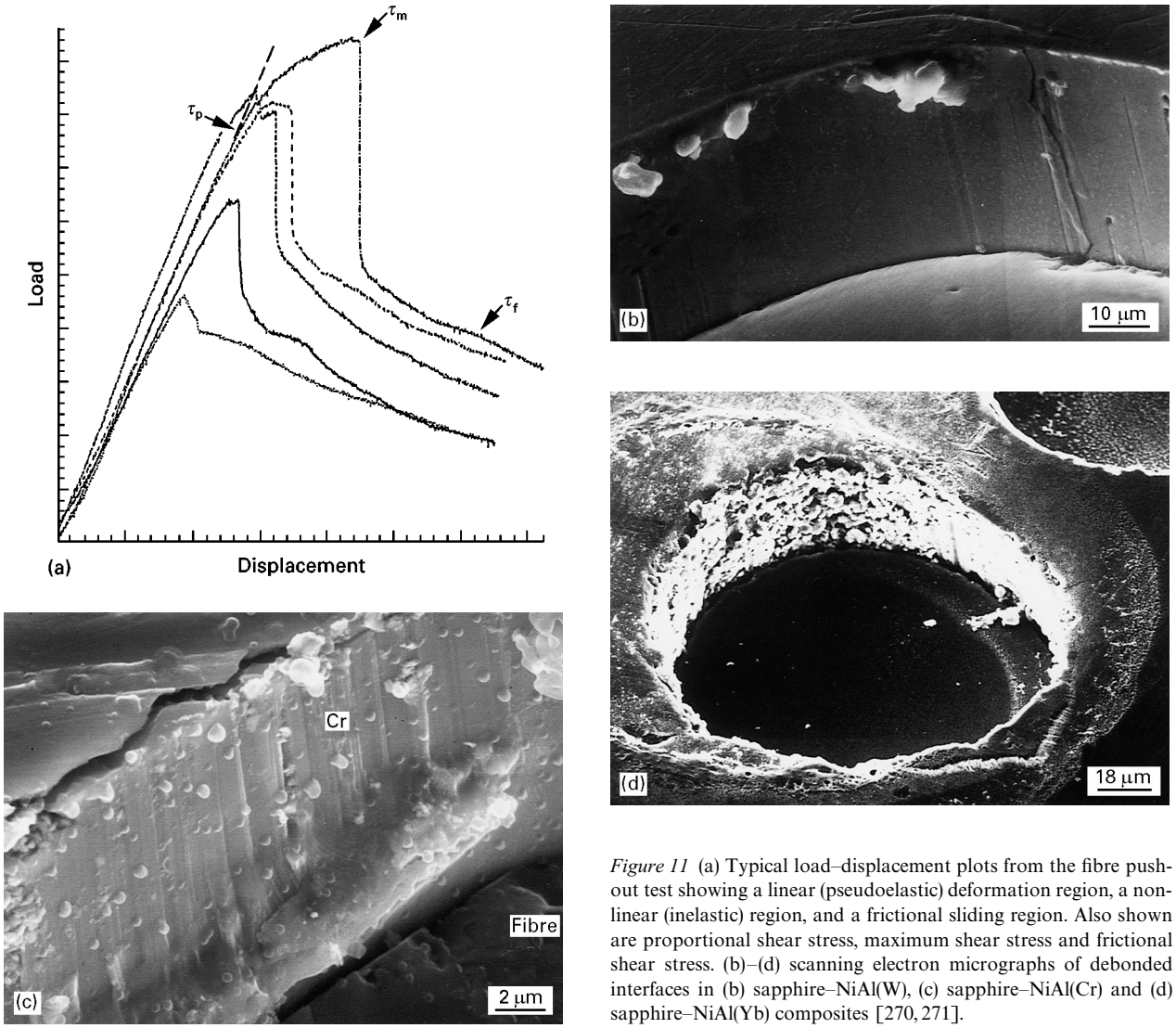

Figure 11 (a) Typical load–displacement plots from the fibre push-out test showing a linear (pseudoelastic) deformation region, a non-linear (inelastic) region, and a frictional sliding region. Also shown are proportional shear stress, maximum shear stress and frictional shear stress. (b)–(d) scanning electron micrographs of debonded interfaces in (b) sapphire–NiAl(W), (c) sapphire–NiAl(Cr) and (d) sapphire–NiAl(Yb) composites [270, 271].

TABLE I Interface strength measurements in liquid-phase processed sapphire–NiAl composites using the fibre push-out technique [323] (the mean shear stress and standard deviation values are listed; the symbol $>$ preceding a value indicates that some fibres could not be debonded during the fibre push-out test within the loading capacity of the machine, and the shear stress value is greater than the value shown)

Matrix	Fabrication method	Interfacial debond shear stress (MPa)	Frictional stress (MPa)
Stoichiometric NiAl	Powder cloth	42 ± 21	22 ± 9
Stoichiometric NiAl	Zone directional solidification of powder-cloth feed material	$> 138 \pm 62$	27 ± 7
NiAl(Yb)	Powder cloth	$> 205 \pm 69$	126 ± 16
NiAl(Yb)	Zone directional solidification of powder-cloth feed material	67 ± 44	53 ± 41
Stoichiometric NiAl	Vacuum induction melting and casting	133 ± 79	48 ± 10
NiAl(Cr)	Vacuum induction melting and casting	154 ± 55	72 ± 39
NiAl(Cr)	Zone directional solidification of as cast feed material	$> 155 \pm 41$	72 ± 35
NiAl(W)	Vacuum induction melting and casting	$> 168 \pm 71$	41 ± 24
NiAl(W)	Zone directional solidification of as cast feed material	$> 159 \pm 69$	28 ± 13

stresses depend upon specimen geometry and test configuration); experimental measurements coupled with appropriate stress analyses are, therefore, necessary to estimate the interface strength. Another approach based upon the measurements of fracture energy is used to estimate the work W_{ad} of adhesion between dissimilar materials [114, 115]. However, as chemical segregation affects W_{ad}, and as interfacial

roughness provides crack shielding and plastic deformation at the interfacial region, the fracture energy approach is difficult to apply (the method usually overestimates W_{ad}).

In summary, the fibre–matrix interface represents a transition region between two monolithic phases (fibre and matrix) whose properties (strength, adhesion, chemistry, structure and topological features) control the stress transfer and load-bearing characteristics of the material. In spite of the extreme sensitivity of interfaces to a myriad of material and test variables, and the inherent thermodynamic instability of interfaces between dissimilar materials, considerable progress has been made in understanding, modelling and tailoring the interface at the microstructural, crystallographic and atomic levels. This progress has resulted primarily from interactions between processing science and surface engineering. Future developments are likely to focus on techniques for *in-situ* characterization of interfaces under service conditions (e.g., *in-situ* measurements of interface strength in reactive environments and/or at elevated temperatures), development of criteria for selecting stress-absorbing compliant layers, prediction and control of fibre degradation by judicious design of fibre and matrix chemistries, by surface engineering, and by controlling fabrication conditions, continued development and refinement of theoretical models which integrate the thermodynamics and kinetics of interfaces with their micromechanical behaviour and, finally, integration of our understanding of interfacial phenomena into manufacturing processes for producing composites with engineered interfaces.

Acknowledgements

An early draft of this paper was prepared at the Lewis Research Center, National Aeronautics and Space Administration (NASA), Cleveland, with financial support from NASA and the National Research Council, Washington, DC. Appreciation is expressed to Thomas K. Glasgow, Chief, Processing Science and Technology Branch, Lewis Research Center, and S. N. Tewari, Professor, Cleveland State University, Cleveland, for support. Support received from the University of Wisconsin-Stout during preparation of the final manuscript is also gratefully acknowledged.

References

1. A. K. MISRA, Compos. Sci. Technol. **50** (1994) 37.
2. A. K. MISRA and R. R. BOWMAN, *Mater. Sci. Engng* **A196** (1995) 197.
3. A. G. METCALFE, in "Interfaces in Metallic Matrix Composites", edited by K. C. Kreider (Academic Press, New York, 1974) p. 269.
4. A. G. METCALFE and M. J. KLEIN, in "Composite Materials", Vol. 1 (Academic Press, New York, 1974) p. 13.
5. S. OCHIAI and K. OSAMURA, *Metall. Trans. A* **18** (1987) 673.
6. S. OCHIAI and K. OSAMURA, *J. Mater. Sci.* **23** (1988) 886.
7. I. H. KHAN, *Metall. Trans. A* **7** (1976) 1281.
8. S. J. BAKER and W. BONFIELD, *J. Mater. Sci.* **13** (1978) 1329.
9. A. OKURA, E. NAKATA and S. SADAI, *J. Jpn Inst. Metals* **47** (1983) 249.
10. S. KOHARA and N. MUTO, *ibid.* **45** (1981) 411.
11. S. DRAPER and I. E. LOCCI, *J. Mater. Res.* **9** (1994) 1397.
12. P. MARTINEAU, R. PAILLAR, M. LAHARE and R. NASLAIN, *J. Mater. Sci.* **19** (1984) 274.
13. H. LIU, U. MADALENO, T. SHINODA, Y. MISHIMA and T. SUZUKI, *ibid* **25** (1990) 4247.
14. L. E. MURR, Interfacial Phenomena in Metals and Alloys (Addison-Wesley, Reading, MA, 1975).
15. H. P. GREENSPAN, *J. Fluid Mech.*, **84** (1978) 125.
16. W. A. ZISMAN, *Adv. Chem.* **43** (1964) 1.
17. A. B. D. CASSIE, *Discuss. Faraday Soc.* **3** (1948) 1.
18. A. W. NEUMANN and R. J. GOOD, *J. Colloid Interface Sci.* **38** (1972) 311.
19. P. G. DEGENNES, *Rev. Mod. Phys.* **57** (1985) 827.
20. J. C. AMBROSE, M. G. NICHOLAS and A. M. STONEHAM, *Acta Metall. Mater.* **40** (1992) 2483.
21. P. JOOS, P. VAN REMOORTERE and M. BRACKE, *J. Colloid Interface Sci.* **136** (1990) 189.
22. I. RIVOLLET, D. CHATAIN and N. EUSTATHOPOULOS, *J. Mater. Sci.* **25** (1990) 3179.
23. S. J. HITCHCOCK, N. T. CARROL and M. G. NICHOLAS, *ibid.* **16** (1981) 714.
24. R. N. WENZEL, *Ind. Engng Chem.* **28** (1936) 988.
25. X. B. ZHOU and J. TH. M. DE HOSSON, *J. Mater. Res.* **10** (1995) 1984.
26. R. P. VOITOVICH, YU. V. NAIDICH and G. A. KOLESNICHENKO, *Poroshk. Metall.*, **6** (1992) 40 English translation, *Powder Metall USSR*, **6** (1992) 494
27. V. DE JONGHE and D. CHATAIN, *Acta Metall. Mater.* **43** (1995) 1505.
28. M. MORRA, E. OCCHIELO and F. GARBASSI, *Prog. Surf. Sci.* (1990) 79.
29. J. GAYDOS and A. W. NEUMANN, *J. Colloid Interface Sci.* **120** (1987) 76.
30. M. A. FORTES, *ibid.* **100** (1984) 17.
31. G. R. WICKHAM and S. D. R. WILSON, *ibid.* **51** (1975) 189.
32. G. R. LESTER, *J. Colloid Sci.* **16** (1961) 315.
33. G. J. JAMESON and M. G. DELCERRO, *J. Chem. Soc., Faraday Trans.* **72** (1976) 883.
34. J. H. AHN, N. TERAO and A. BERGHEZEN, *ibid.* **22** (1988) 793.
35. S. M. DEVINCENT, D. L. ELLIS and G. M. MICHAL, NASA Contractors' Report 187087 (1991).
36. B. CHALMERS and R. H. WADIE, *J. Inst. Metals* **66** (1940) p. 241.
37. G. L. J. BAILEY and H. C. WATKINS, *ibid.* **80** (1951–1952) 57.
38. J. G. LI and H. HAUSNER, *J. Mater. Sci. Letters*, **10** (1991) 1275.
39. G. V. SAMSANOV, A. D. PANASYUK and G. K. KOZINA, *Sov, Powder Metall. Metal Ceram.* **71** (1968) 874.
40. P. T. VIANCO and D. R. FREAR, *J. Metals* **7** (1993) 14.
41. T. CHOH and T. OKI, *Mater. Sci. Technol.* **3** (1987) 378.
42. T. CHOH, R. KAMMEL and T. OKI, *Z. Metallkde* **78** (1987) 286.
43. J. V. NAIDICH, *Prog. Surf. Membrane Sci.* **14** (1981) 353.
44. JU. V. NAIDICH, V. S. ZHURAVLOV and N. I. FRUMINA, *J. Mater. Sci.* **25** (1990) 1895.
45. YU. V. NAIDICH, Y. N. CHUBASHOV, N. F. ISCHUK and V. P. KRASOVSKI, *Poroshk. Metallurgiya* **246** (1983) 67.
46. G. V. SAMSANOV and I. M. VINITSKI, "Handbook of Refractory Compounds (IFI–Plenum, New York, 1980).
47. N. EUSTATHOPOULOS, *Int. Metalls. Rev.* **28** (1983) 189.
48. N. EUSTATHOPOULOS, J. C. JOUD, P. DESRE and J. M. HICTER, *J. Mater. Sci.* **9** (1974) 1233.
49. N. EUSTATHOPOULOS and L. COUDURIER, *J. Adhes. Sci. Technol.* **6** (1992) p. 1011.
50. N. EUSTATHOPOULOS, D. CHATAIN and L. COUDURIER, *Mater. Sci. Engng* **A135** (1991) 83.
51. D. R. H. JONES, *J. Mater. Sci.* **9** (1974) 1.
52. B. C. ALLEN and W.D . KINGERY, *Trans. Metall. Soc. AIME* **215** (1959) 30.
53. J. M. HOWE, *Int. MNater. Rev.* **38** (1993) 233.
54. J. G. LI and H. HAUSNER, *Mater. Lett.* **14** (1992) 329.

55. J. G. LI and H. HAUSNER, *J. Eur. Ceram. Soc.* **9** (1992) 101.
56. C. MARUMO and J. A. PASK, *J. Amer. Ceram. Soc.* **60** (1977) 276.
57. G. G. GNESIN and A. I. RAICHENKO, *Poroshk. Metall.* **5** (1973) 35.
58. V. N. ERMENKO and YU. V. NAIDICH, *Russ. J. Inorg. Chem.* **4** (1959) 931.
59. P. NIKOLOPOULOS, S. AGATHOPOULOS, G. N. ANGELOPOULOS, A. NAOUMIDIS and H. GRUBMEIER, *J. Mater. Sci.* **27** (1992) 139.
60. J. G. LI and H. HAUSNER, *Scripta Metall. Mater.* **32** (1995) 377.
61. T. R. JONAS, J. A. CORNIE and K. C. RUSSEL, *Metall. Mater. Trans A* **26** (1995) 1491.
62. T. J. WHALEN and A. T. ANDERSON, *J. Amer. Ceram. Soc.* **58** (1975) 396.
63. K. NOGI and K. OGINO, in Proceedings of the symposium on Advanced Structural Materials, edited by D. S. Wilkinson (Pergamon, Oxford, 1988) p. 97.
64. J. V. NAIDICH and V. CHUVASHOV, *J. Mater. Sci.* **18** (1983) 2071.
65. C. ZHONGYU, W. JIMBO and H. XIANGUI, in "Interfaces in metal ceramic composites", edited by R. Y. Lin *et al.* (1988) p. 233.
66. K. KUNIYA and H. ARAKAWA, US Patent 3 871 834 (1975).
67. R. V. SARA, US Parent 4 347 083 (1983).
68. M. NICHOLAS and D. MORTIMER, in Proceedings of the International Conference on Carbon Fibers, *Their Composites and Applications* (Plastics Institute, London, 1971) p. 129.
69. K. NOGI, Y. OSUGI and K. OGINO, *Iron Steel Inst. Jpn* **30** (1990) 64.
70. N. KISHAPOROV, V. CHENTSOV, I. FRISHBERG and V. PASTUKHOV, *Sov. Powder Metall. Metal Ceram.* **11** (1984) 869.
71. R. W. SEXTON and D. M. GODDARD, US Patent 4 341 823 (1982).
72. W. CHENGFU, MEIFANG and Y. DUOFENG, in Proceedings of the Sixth International Conference on Composite Materials, edited by F. L. Mathews *et al.* (Elsevier, Amsterdam, 1987) p. 2.183.
73. H. KATZMAN, US Patent 4 376 803 (1983).
74. H. KATZMAN, *J. Mater. Sci.* **22** (1987) 144.
75. K. FUJITA, Y. SAWADA and K. HONJO, *J. Jpn Soc. Compos. Mater.* **17** (1991) 80.
76. P. ROCHER, J. M. QUENISSET and R. NASLAIN, *J. Mater. Sci. Lett.*, **4** (1985) 1527.
77. I. L. KALNIN, US Patent 4 056 874 (1977).
78. K. I. PORTNOI, USSR Patent 5 599 85 (1977).
79. A. P. LEVITT, E. DICESARE and S. M. WOLF, *Metall. Trans.* **3** (1972) 2455.
80. R. T. PEPPER and E. G. KENDALL, US Patent 4 082 864 (1978).
81. O. REMONDIER, R. PAILLAR, R. MAMODE and PH. ROY in "Developments in Science and Technology of Composite Materials", edited by A. R. Bunsell *et al.* (1985) p. 732.
82. B. C. PAI and P. K. ROHATGI, *Mater. Sci. Engng* **21** (1975) 161.
83. B. KINDL, Y. L. LIU, E. NYBERG and N. HANSON, *Composite Sci. Technol* **43** (1992).
84. M. UEKI, M. NAKA and I. OKAMOTO, *J. Mater. Sci. Lett.* **5** (1986) 1261.
85. L. COUDURIER and N. EUSTATHOPOULOS, *J. Mater. Sci.* **24** (1989) 1109.
86. A. BARDAL and R. HOEIER, Government Research Annual Index PB92-102904/XAB, May 1991 (Metals Abstract, March 1992) 187.
87. M. SHIMBO, M. NAKA and I. OKAMOTO, *J. Mater. Sci. Lett.* **8** (1989) 663.
88. S K. RHEE, *J. Amer. Ceram. Soc.* **54** (1971) 376.
89. R. D. CARNAHAM, T. L. JOHNSON and C. H. LI, *J. Amer. Ceram. Soc.* **41** (1958) 343.
90. H. JOHN and H. HAUSNER, *Int. J. High Tech Ceram.* **2** (1986) 73.
91. J. GOICOECHEA, G. CORDAVILLA, E. LOIUS and A. PAMIES, *Scripta Metall. Mater.* **25** (1991) 479.
92. M. NICHOLAS, P. R. D. FORGAN and D. M. POOLE, *J. Mater. Sci.* **3** (1968) 9.
93. M. NICHOLAS, *J. Mater. Sci.* **5** (1970) 571.
94. N. I. ABDUL-LATTEF, A. R. I. KHEDAR and S. K. GOEL, *J. Mater. Sci. Lett.* **5** (1970) 571.
95. A. BANERJI, P. K. ROHATGI, W. REIF, *Metallweissenschaft Technik*, **38** (1984) 356.
96. S. Y. OH, Ph.D. Dissertation, Massachusetts Institute of Technology, Cambridge, MA (1987).
97. R. WARREN and C. H. ANDERSON, *Composites* **15** (1984) 101.
98. A. MORTENSEN, *Mater. Sci. Engng.* **A135** (1991) 1.
99. F. DELANNAY, L. FROYEN and A. DERUYTTERE, *J. Mater. Sci.* **22** (1987) 1.
100. R. ASTHANA and S. N. TEWARI, *Compos. Manuf.* **4** (1993) 3.
101. V. LAURENT, PhD Thesis, Grenoble (1988).
102. N. EUSTATHOPOULOS and B. DREVET, *Compos. Interfaces* **2** (1994) 29.
103. V. LAURENT, D. CHATAIN and N. EUSTATHOPOULOS, *Mater. Sci. Engng* **A135** (1991) 89.
104. J. LI, *Ceram. Int.* **20** (1994) 391.
105. M. HUMENIK, Jr and W. D. KINGERY, *J. Amer. Ceram. Soc.* **37**(1) (1954) 18.
106. J. F. MCDONALD and J. G. EBERHART, *Trans. AIME* **233** (1965) 512.
107. S. N. OMENYI and A. W. NEUMANN, *J. Appl. Phys.* **47** (1976) 3956.
108. A. W. NEUMANN, R. J. GOOD, C. J. HOPE and M. SEJPAL, *J. Colloid Interface Sci.* **49** (1974) 291.
109. S. N. OMENYI. R. P. SMITH and A. W. NEUMANN, *ibid.* **75** (1980) 117.
110. D. M. STEFANESCU, A. MOITRA, A. S. KACAR and B. K. DHINDAW, *Metall. Trans. A* **21** (1990) 231.
111. R. ASTHANA, *Metall. Trans. A.* **25** (1994) 225.
112. R. ASTHANA, *J. Colloid Interface Sci.* **165** (1994) 256.
113. P. F. AUBORG,, PhD Dissertation, Massachusetts Institute of Technology, Cambridge, MA (1976).
114. A. G. EVANS, M. RUHLE, B. J. DALGLEISH and P. G. CHARALAMBIDES, *Mater. Sci. Engng* **A126** (1990) 53.
115. *Idem. Metall. Trans. A* **21** (1990) 2419.
116. A. R. MIEDEMA and R. BOOM, *Z. Metallkde* **69** (1978) 183.
117. ,A. R. MIEDEMA and F. J. A. DE BROEDER, *ibid.* **70** (1979) 14.
118. A. ALONSO, A. PAMIES, J. NARCISCO, C. GARCIA-CORDOVILLA and E. LOUIS, *Metall. Trans. A* **24** (1933) 1423.
119. F. P. CHIARAMONTE and B. N. ROSENTHAL, *J. Amer. Ceram. Soc.* **74** (1991) 658.
120. H. FUJI, H. NAKAE and K. OKADA, *Acta Metall. Mater.* **41** (1993) 2963.
121. H. FUJI, H. NAKAE and K. OKADA, *Metall. Trans A* **24** (1993) 1391.
122. C. R. MANNING and T. B. GURGANUS, *J. Amer. Ceram. Soc.* **52** (1969) 115.
123. H. FUKUNAGA and K. GODA, *Bull. Jpn Sol. Mech. Engng.* **27** (1984) 1245.
124. B. N. K. RAM, P. K. ROHATGI, R. ASTANA and K. G. SATYANARAYANA, in "Solidification of Metal matrix Composites," edited by P. Rohatgi (1990) p. 151.
125. R. MEHRABIAN, R. G. RIEK and M. C. FLEMINGS, *Metall. Trans.* **5** (1974) 1899.
126. S. W. IP, M. KUCHANSKI and J. M. TOGURI, *J. Mater. Sci. Lett.* **12** (1993) 1699.
127. F. ERNST, *Mater. Sci. Engng* **A14** (1995) 97.
128. H. F. FISCHMEISTER, in "Ceramic Microstructures, role of Interfaces", edited by J. A. Pask and A. G. Evans (Plenum, New York, 1986).
129. J. P. ROCHER, F. GIROT, J. M. QUNISSET, R. PAILLAR and R. NASLIN, *Mem. Etudes Sci. Rev. Metall.* Feb. (1986) 69.
130. U. GANGOPADHYAYA and P. WYNBLATT, *J. Mater. Sci.* **30** (1995) 94.

131. R. ASTHANA and P. K. ROHATGI, *Compos. Manuf.* **3** (1992) 119.
132. M. F. AMATEAU, *J. Compos. Mater.* **10** (1976) 279.
133. T. W. CHOU, A. KELLY and A. OKURA, *Composites* **16** (1985) 187.
134. A. G. KULKARNI, B. C. PAI and N. BALASUBRAMANIAN, *J. Mater. Sci.* **14** (1979) 592.
135. P. ROHATGI and R. ASTHANA, in "Controlled Interphases in Composite Materials", edited by H. Ishida (Elsevier, New York, 1990) p. 637.
136. J. A. ISSACS, F. TARICCO, V. MICHAUD and A. MORTENSEN, *Metall. Mater. Trans. A* **22** (1991) 2855.
137. S. NOURBAKHSH, O. SAHIN, W. H. RHEE and H. MARGOLIN, *ibid.* **22** (1991), 3059.
138. A. E. W. JARFORS, L. SVENDSEN, M. WALLIDER and H. FREDRIKSSON, *Metall. Trans. A* **24** (1993) 2577.
139. I. W. HALL, *Metallography* **20** (1987) 237.
140. S. KUDELA, V. GERGELY, E. JANSCH, A. HOFMAN, S. BAUNACK, S. OSWALD and K. WETZIG, *J. Mater. Sci.* **29** (1994) 5576.
141. J. F. MASON, C. M. WARWICK, P. J. SMITH, J. A. CHARLES and T. W. CLYNE, *ibid.* **24** (1989) 3934.
142. S. M. DEVINCENT and G. M. MICHAL, *Metall. Trans. A* **24** (1993) p. 53.
143. G. D. ZHANG, S. R. FENG, Q. LI, J. T. BLUCHER and J. A. CORNIE, "Controlled Interphase in Composite Materials", edited by H. Ishida (Elsevier, New York, 1990).
144. E. IGNATOWITZ, *Aluminium* **50** (1974) 334.
145. D. A. WEIRAUCH Jr, W. M. BALABA and A. J. PEROTTA, *J. Mater. Res.* **10** (1995) 640.
146. A. A. BAKER, C. C. SHIPMAN and P. W. JACKSON, *Fiber Sci. Tech* **5** (1972) 213.
147. W. L. LACHMAN, R. A. PENTY and A. F. JAHN, US Patent 3 860 443 (1975).
148. T. G. NIEH and A. E. VIDOZ, *J. Amer. Ceram. Soc.* **65** (1982) 227.
149. A. MIYASE and K. PIEKARSKI, *J. Mater. Sci.* **16** (1981) 251.
150. *Idem.*, *J. Compos. Mater.* **14** (1980) 160.
151. K. I. PORTNOI, USSR Patent 559985 (1977).
152. A. KLEINE and H. J. DUDEK, in "Magnesium Alloys and Their Applications" (Deutsche Gesellschatt für Metallkunde Informationgesselschaft, Darmstadt, 1992) p. 447.
153. S. G. WARRIER, C. A. BLUE and R. Y. LIN, *J. Mater. Sci.* **28** (1993) 760.
154. M. DE SANCTIS, S. PELLELIER, Y. BIENVENU and H. VINCENT, *ibid.* **29** (1994) 356.
155. H. RIBES, M. SUERY, G. L. ESPERANCE and J. G. LEGOUX, *Metall. Trans. A.* **21** (1990) 2489.
156. D. J. TOWLE and C. M. FREIND, *Scripta Metall.* **26** (1992) 437.
157. R. C. BOEHM and A. BANERJEE, *J. Chem. Phys.* **96** (1992) 1150.
158. S. D. PETEVES, P. TAMUYSEV, P. HELBACH, M. AUDIER, V. LAURENT and D. CHATAIN, *J. Mater. Sci.* **25** (1990) 3765.
159. M. KOBASHI, T. MOHRI and T. CHOH, *J. Mater. Sci.* **28** (1993) p. 5707.
160. W. KOHLER, *Aluminium* **51** (1975) 443.
161. D. S. HAN, H. JONES and H. V. ATKINSON, *J. Mater. Sci.* **28** (1993) 2654.
162. J. NARCISCO, A. ALONSO, A. PAMIES, C. GARCIA-CORDOVILLA and E. LOUIS, *Scripta Metall. Mater.* **31** (1994) 1495.
163. K. KOBASHI and T. CHOH, *J. Mater. Sci.* **28** (1993) 684.
164. V. LAURENT, D. CHATAIN and N. EUSTATHOPOULOS, *J. Mater. Sci.* **22** (1987) 244.
165. V. LAURENT, D. CHATAIN, N. EUSTATHOPOULOS and X. DUMANT, in "Cast Reinforced Metal Composites", edited by S. G. Fishman and A. K. Dhingra (American Society for Metals, Metals Park, OH, 1988) p. 27.
166. S. Y. OH, J. A. CORNIE and K. C. RUSSELL, *Metall. Trans A* **20** (1989) 527.
167. *Idem.*, *ibid* **20** (1989) 533.
168. B. DREVET, S. KALOGEROPOULOS and N. EUSTATHOPOULOS, *Acta Metall. Mater.* **41** (1993) 3119.
169. R. ASTHANA and P. K. ROHATGI, *Z. Metallkde* **83** (1992) 887; **84** (1993) 44.
170. T. F. STEPHENSON and J. A. E. BELL, in Proceedings of the Conference in Advances in Synthesis and Processes, (Society for the Advancement of Material and Process Engineering, Azusa, CA, 1992) p. 560.
171. H. YUMOTO, A. TAKAHASHI and N. IGATA, in Proceedings of the Conference in Advanced Materials for Future Industries (International Convention Management, Inc., 1991) p. 737.
172. R. J. ARSENAULT, *Composites* **25** (1994) p. 540.
173. W. C. MOSHIER, J. S. AHEARN and D. C. COOKE, *J. Mater. Sci.* **22** (1987) 115.
174. K. L. CHOY, *Scripta Metall. Mater.* **32** (1995) 219.
175. C. CAROTENUTO, A. GALLO and L. NICOLAIS, *J. Mater. Sci.* **29** (1994) 4967.
176. K. SUGANUMA, *J, Mater. Res.* **8** (1993) 2569.
177. M. KOBASHI and T. CHOH, *J. Mater. Sci.* **28** (1993) 684.
178. M. SUERY, G. L. 'ESPERANCE, B. D. HONG, L. N. THANH and F. BORDEAUX, *J. Mater. Engng Performance* (1993) 365.
179. K. S. FOO, W. M. BANKS, A. J. CRAVEN and A. HENDY, *Composites* **25** (1994) 677.
180. J. C. VIALA, F. BOSSELET, V. LAURENT and Y. LEPETITCORPS, *J. Mater. Sci.* **28** (1993) 5301.
181. Y. L. LIU and B. KINDL, *Scripta Metall. Mater.* **27** (1992) 1367.
182. B. INEM and G. POLLARD, *J. Mater. Sci.* **28** (1993) 4427.
183. A. BARDAL, *Mater. Sci. Engng* **A159** (1992) 119.
184. D. J. LLOYD, *Int. Mater. Rev.* **39** (1994) 1.
185. A. BARDAL and R. HOIER, in "Metal-matrix Composites: Processing, Microstructure and Properties" (Risø National Laboratory, Risø, Roskulde, 1991) p. 205.
186. J. NARCISCO, C. GARCIA-CORDOVILLA and E. LOUIS, *Mater. Sci. Engng* **B15** (1992) 148.
187. D. J. LLYOD, M. P. LAGACE and M. D. MCLEOD, in "Controlled Interphases in Composite Materials" edited by H. Ishida (Elsevier, Amsterdam, 1990).
188. J. C. VIALA, P. FORTIER and J. BOUIX, *J. Mater. Sci.* **25** (1990) 1842.
189. D. M. DIGNARD-BAILY, T. F. MALIS, J. D. BOYD and J. D. EMBURY, in Proceedings of the Symposium on Advanced Structural Materials edited by D. S. Wilkinson (Pergamon, Oxford, 1989) p. 87.
190. X. DUMANT, E. BEANGON and REGAZZONI, *J. Metals* **41** (1989) 45.
191. D. LEE, M. D. VARDIN, C. A. HANDWERKER and U. R. KATTNER, *Mater. Res. Sci. Symp. Proc.* **120** (1988) 357.
192. K. KANNIKESWARAN and R. Y. LIN, in Proceedings of the Symposium on Advanced Structural Materials, edited by D. S. Wilkinson (Pergamon, Oxford, 1988) p. 79.
193. M. KH. SHORSHOROV, T. A. CHERNYSHOVA and L. I. KOBELEVA, in Proceedings of the Fourth International Conference on Composite Materials, edited by T. Hagashi *et al.* (Japan Society for Composite Materials, Tokyo, 1982) p. 849.
194. J. C. ROMERO and R. J. ARSENAULT, *Acta Metall. Mater.* **43** (1995) 849.
195. T. CHERNYSHOVA and A. V. REBROV, *J. Less-Common Metals* **117** (1980) 203.
196. T. ISEKI, T. KAMEDA and T. MARUYAMA, *J. Mater. Sci.* **19** (1984) 1692.
197. D. J. LLOYD and E. DEWING, Proceedings the Symposium on Advanced Structural Materials, edited by D. S. Wilkinson (Pergamon, Oxford, 1988) p. 71.
198. R. WARREN and C. LI, in "Controlled Interphases in Composite Materials", edited by H. Ishida (Pergamon Oxford, Metullurgical Society of AIME, Warrendale, PA, 1988) p. 583.
199. R. Y. LIN and K. KANNIKESWARAN, in "Interfaces in Metal–ceramic Composites", edited by R. Y. Lin, R. J. Arsenault, G. P. Martins and S. G. Fishman, (Metallurgical Society of AIME, Warrendale, PA, 1989) p. 153.

200. L. CAO, L. GENG, C. K. YAO and T. C. LEI, *Scripta Metall.* **23** (1989) 227.
201. A. E. HUGHES, M. M. HEDGES and B. A. SEXTON, *J. Mater. Sci.* **25** (1990) 4856.
202. J. E. RESTALL, A. BURNWOOD-SMITH and K. F. A. WALLES, *Metals Mater.* **4** (1970) 467.
203. L. N. THANH and M. SUERY, *Scripta Metall. Mater.* **25** (1991) 2781.
204. J. NARCISCO, C. GARCIA-CORDAVILLA and E. LOUIS, *Mater. Sci. Engng* **B15** (1992) 148.
205. T. R. BREVIK and K. PETTERSON, in "Interfacial Phenomena in Composite Materials '91," edited by I. Verpoest and F. Jones (Butterworth-Heinemann, Oxford, 1991) p. 219.
206. L. ESPIE, B. DREVET and N. EUSTATHOPOULOS, *Metall. Trans. A*, **25** (1994) 599.
207. K. M. PREWO and G. MCCARTHY, *J. Mater. Sci.* **8** (1972) 919.
208. D. J. LLOYD, H. LAGACE, A. MCLEOD and P. L. MORRIS, *Mater. Sci. Engng* **A107** (1989) 73.
209. S. KOHARA, Society for the Advancement of Material and Process Engineering, Azusa, CA, Composite Materials, edited by Kawata and Akesaha, Proceeding US-Japan Conference on (Japan Society for Compos. Maters., Tokyo, 1981) p. 224.
210. Y. FLOM and R. J. ARSENAULT, *Mater. Sci. Engng* **77** (1986) 191.
211. E A. FEEST, *Composites* **25** (1994) 75.
212. T. ISEKI, T. KAMEDA and T. MARUYAMA, *J. Mater. Sci.* **19** (1984) 1692.
213. X. DUMANT, E. BEAUGNON and G. REGAZZONI, *J. Metals* (1984) 46.
214. K. YOSHII, S. INOUE, S. INAMI and H. KAWABE, *J. Mater. Sci.* **24** (1989) 3069.
215. H. MORIMOTO and G. OHUCHI, *J. Iron Steel Inst. Japan* **75** (1989) 1541.
216. B. KINDL, Y. H. TENG and Y. L. LU, *Composites* **25** (1994) p. 671.
217. J. M. YANG and S. Y. JENG, *J. Metals* **41** (1989) 56.
218. R. PAILLAR, P. MARTINEAU, M. LAJOYE, Y. LE PETITCORPS and R. NASLAIN, in "Reactivity of Solids", Part B, edited by P. Barrett and L. Dufour (Elsevier, New York, 1985) p. 113.
219. D. B. GUNDEL and F. E. WAWNER, *Scripta Metall. Mater.* **25** (1991) 437.
220. C. G. RHODES and R. A. SPURLING, in "Recent Advances in Composites in the US and Japan", edited by R. Visnon and M. Taya (American Society for Testing and Materials, Philadelphia, PA, 1985) p. 585.
221. D. WEBSTER, *Metall. Trans. A.* **13** (1982) 1511.
222. R. T. SWAN and D. M. EASTERLING, *Composites*, **15** (1984) 305.
223. V. LAURENT, D. CHATAIN, C. CHATTILLON and N. EUSTATHOPOULOS, *Acta Metall. Mater.*, **36** (1988) 1797.
224. D. J. WANG and S. T. WU, *ibid.* **42** (1994) 4029.
225. A. C. D. CHAKLADER, A. M. ARMSTRONG and S. K. MISRA, *J. Amer. Ceram. Soc.* **51** (1968) 630.
226. A. C. D. CHAKLADER and S. P. MEHROTRA, *Metall. Trans.* **16B** (1985) 567.
227. J. J. BRENNAN and J. A. PASK, *J. Amer. Ceram. Soc.* **51** (1968) 569.
228. M. GUNDUZ and J. D. HUNT, *Acta Metall.* **37** (1989) 1839.
229. H. JOHN and H. HAUSNER, *J. Mater. Sci. Lett.* **5** (1986) 549.
230. J. A. CHAMPION, B. J. KEENE and J. M. SILWOOD, *J. Mater. Sci.* **4** (1969) 39.
231. Z. LIJUN, W. JINBO, Q. JITLING, N. QIU and Q. PEIXIANG, in "Interfaces in Metal-ceramic Composites", edited by R. Y. Lin, R. J. Arsenault, B. P. Martins and S. G. Fishman (Metallurgical Society of AIME, Warrendale, PA, 1989) p. 213.
232. S. K. RHEE, *Mater. Sci. Engng* **16** (1974) 45.
233. R. D. CARNAHAM, T. L. JOHNSTON and C. H. LI, *J. Amer. Ceram. Soc.* **41** (1958) 343.
234. S. M. WOLF, A. P. LEVITT and J. BROWN, *Chem. Engng Prog.* **62** (1966) 74.
235. C. BERAUD, M. COURBIERE, C. ESNOUF, D. JUVE and D. TREHEUX, *J. Mater. Sci.* **24** (1989) 4545.
236. T. NINOMIYA and T. CHOH, *J. Jpn Inst. Light Metals* **41** (1991) 528.
237. U. MADELENO, H. LIU, T. SHINODA, Y. MISHIMA and T. SUZUKI, *J. Mater. Sci.* **25** (1990) 3273.
238. P. K. ROHATGI, R. ASTHANA and S. DAS, *Int. Metall. Rev.* **31** (1986) 115.
239. P. K. P. K. ROHATGI, S. RAY, R. ASTHANA and C. S. NARENDRANATH, *Mater. Sci. Engng* **A162** (1993) 163.
240. C. GARCIA-CORDAVILLA, E. LOUIS and A. PAMIES, *J. Mater. Sci.* **21** (1986) 2787.
241. J. J. DUDEK, A. KLEIN, R. BORATH and G. NEITZ, *Mater. Sci. Engng* **A167** (1993) 129.
242. C. S. KANETKAR, A. S. KACAR and D. M. STEFANESCU, *Metall. Trans. A* **19** (1988) 1833.
243. *J. Mater. Sci.* **28** (1993) 1317.
244. D. XU, D. WAG and D. LIN, *ibid* **28** (1993) 599.
245. CHENN and FANN, *Metal Abstracts* (1992) 264.
246. G R. CAPPLEMAN, J. F. WATTS and T. W. CLYNE, *J. Mater. Sci.* **20** (1985) 2159.
247. A. MUNITZ, M. METZGER and R. MEHRABIAN, *Metall. Trans. A* **10** (1979) 1491.
248. J. J. DUDEK, A. KLEIN, R. BORATH and G. NEITE, *Mater. Sci. Engng* **A167** (1993) 129.
249. H. A. KATZMAN, *Mater. Manuf. Processes* **5** (1990) 1.
250. P. R. CHIDAMBARAM, G. R. EDWARDS and D. L. OLSON, *Metall. Mater. Trans. A* **25** (1994) 2083.
251. D. J. LLOYD, I. JIN and G. C. WEATHERLY, *Scripta Metall. Mater.* **31** (1994) 393.
252. F. RAHMAN, S. FOX, H. M. FLOWER and D. R. F. WEST, *J. Mater. Sci.* **29** (1994) 1636.
253. A. MCMINN, R. A. PAGE and W. WEI, *Metall. Trans. A* **18** (1987) 273.
254. J. E. HACK, R. A. PAGE and G. R. LEVERANT, *ibid.* **15** (1984) 1389.
255. B. C. PAI, P. K. ROHATGI, K. V. PRABHAKAR and S. RAY, *Mater. Sci. Engng* **24** (1976) 31.
256. S. RAY, *J. Mater. Sci.* **28** (1993) 5397.
257. S. KUDELA, V. GERGELY, A. SCHWEIGHOFER, S. BAUNACK, S. OSWALD and K. WETZIG, *ibid.* **29** (1994) 5071.
258. HALSTEDT *et al. Mater. Sci. Engng* **A129** (1990) 135.
259. A. R. CHAMPION, W. H. KRUEGER, H. S. HARTMAN and A. K. DHINGRA, in Proceedings of the Second International Conference on Composite Materials, edited B. R. Norton *et al.* (Metallurgical Society of AIME, Warrendale, PA, 1978) p. 883.
260. R. A. PAGE and G. R. LEVERANT, in Proceedings of the Fifth International Conference in Composite Materials edited by W. C. Harrigan *et al.* (Metallurgical Society of AIME, Warrendale, PA, 1985) p. 867.
261. J. NUNES, E. S. C. CHIN, J. M. SLEPETZ and N. TSANGARAKIS, Proceedings of the Fifth International Conference in Composite Materials edited by W. C. Harrigan *et al.* (Metallurgical Society of AIME, Warrendale, PA, 1985) p. 723.
262. S. NOURBAKHSH, O. SAHIN, W. H. RHEE and H. MARGOLI, *Metall. Trans. A.* **25** (1994) 1259.
263. J. A. ISSACS, F. TARICCO, V. J. MICHAUD and A. MORTENSEN, *ibid.* **22** (1991) 2855.
264. R. R. BOWMAN, *Mater. Res. Soc. symp. Proc.* **273** (1992) 145.
265. S. N. TEWARI, R. ASTHANA and R. D. NOEBE, *ibid.* **24** (1993) 2119.
266. R. ASTHANA, S. N. TEWARI and R. R. BOWMAN, *ibid.* **26** (1995) 209.
267. D. XU, D. WANG and D. LIN, *Scient Metall. Mater.* **28** (1993) 599.
268. S. NOURBAKHSH, F L. LIANG and H. MARGOLIN, *Metall. Trans. A* **21** (1990) 2881.
269. A. K. MISRA, Lewis Research Center, NASA Cleveland, OH Countractors Report 4171 (1986).
270. S. N. TEWARI, R. ASTHANA, R. TEWARI, R. BOWMAN and J. SMITH, *Metall. Trans. A* **26** (1995) 477.

271. R. ASTHANA, R. TEWARI and S. N. TEWARI, *Metall. Mater Trans. A* (1995) 2175.
272. M. NICHOLAS, P. R. D. FOLGAR and D. M. POOLE, *J. Mater. Sci.* **3** (1968) 9.
273. M. NICHOLAS, *ibid* **5** (1970) 571.
274. R. WARREN and C. H. ANDERSON, *Composites* **15** (1984) 101.
275. K. SHANKER, L. T. MAVROPOULOS, R. A. L. DREW and P. G. TSANTRIZOV, *Composites* **23** (1992) 47.
276. A. B. GOKHALE, L. LU and R. ABBASCHIAN, in "Solidification of Metal Matrix Composites", edited by P. Rohatgi (Metallurgical Society of AIME, Warrendale, PA, 1990).
277. C. MARUMO and J. A. PASK, *J. Amer. Ceram. Soc.* **60** (1977) 276.
278. K. PRABRIPUTALOONG and M. R. PIGGOT, *J. Electrochem. Soc.* **121** (1974) 430.
279. *Idem. J. Amer. Ceram. Soc.* **56** (1973) 177.
280. A. STANDAGE and M. S. GANI, *J. Amer. Ceram. Soc.* **50** (1967) 101.
281. R. D. LOEHMAN, *Ceram. Bull.* **68** (1989) 891.
282. J. A. YEOMANS and T. F. PAGE, *J. Mater. Sci.* **25** (1990) 2312.
283. C. R. MANNING and T. B. GURGANUS, *J. Amer. Ceram. Soc.* **52** (1969) 115.
284. JU. V. NAIDICH, *Prog. Surf. Membrane Sci.* **14** (1981) 353.
285. A. BANERJEE, P. K. ROHATGI and W. REIF, *Metallurgy* **38** (1984) 656.
286. B. N. K. RAM, P. K. ROHATGI, R. ASTHANA and K. G. SATYANARAYANA, in "Solidification of Metal matrix Composites", edited by P. Rohatgi (Metallurgical Society of AIME, Warrendale, PA, 1990) p. 151.
287. P. NIKOLOPOULOS and D. SORTIROPOULOS, *J. Mater. Sci. Lett.* **6** (1987) 1429.
288. F. J. RITZERT and R. L. DRESHFELD, Lewis Research Center, NASA Cleveland, OH, Technical Memorandum 103901 (1992).
289. T. STEPHENSON, Y. LEPETITCORPS and J. M. QUENISSET, *Mater. Sci. Engng* **A135** (1991) 101.
290. S. A. RICKELS, PhD Dissertation, Georgia Institute of Technology (1992).
291. P. K. ROHATGI, B. C. PAI and S. C. PANDA, *J. Mater. Sci.* **14** (1979) 2277.
292. P. K. ROHATGI, *J. Metals* Nov. (1994) 54.
293. K. SUGANUMA, G. SASAKI and T. FUJITA, in Proceedings of the Sixth Japan Institute of Metals International Intermetallic Compounds: Structure and Mechanical Properties (Japan Institute of Metals, Tokyo, 1991) p. 459.
294. J. HU, W. D. FEI, C. LI and C. K. YAN, *J. Mater. Sci. Lett.* **13** (1994) 1797.
295. M. E. FINE, R. MITRA and J. R. WEERTMAN, *Z. Metallkde* **84** (1993) 282.
296. N. TUNCA, G. N. DELAMORE and R. W. SMITH, *Metall. Trans. A* **21** (1990) 2919.
297. V. G. LEVICH, "Physicochemical Hydrodynamics" (Prentice-Hall, Englewood Cliff, NJ, 1962) 2nd Edn.
298. Y. A. CHANG, R. KIESCHKE, J. DEKOCK and M. X. ZHANG, in "Control of Interfaces in Metal and Ceramic Composites, edited by R. Y. Lin and S. G. Fishman (Metallurgical Society of AIME, Warrendale, PA, 1994) p. 3.
299. L. B. CANTRELL, E. M. CLEVENGER and J. H. PEREPEZKO, in "Control of Interfaces in Metal and Ceramic Composites", edited by R. Y. Lin and S. G. Fishman (Metallurgical Society of AIME, Warrendale, PA, 1994) p. 51.
300. W. SI, P. LI and R. WU, in "Control of Interfaces in Metal and Ceramic Composites", edited by R. Y. Lin and S. G. Fishman (Metallurgical Society of AIME, Warrendale, PA, 1994) p. 81.
301. K. XU, L. WANG and R. J. ARSENAULT, in "High Performance Composites-commonality of Phenomena", edited by K. K. Chawla, P. K. Liaw and S. G. Fishman (Metallurgical Society of AIME, Warrendale, PA, 1994) p. 155.
302. T. C. CHOU and T. G. NIEH, *Scripta Metall. Mater.* **25** (1991) 2059.
303. V. MASSARDIER, P. KERDELHUE, P. MERLE and J. BESSON, *Mater. Sci. Engng* **A191** (1995) 267.
304. M. RUHLE and A. G. EVANS, *Mater. Res. Soc. Symp. Proc.* **120** (1988) 293.
305. M. PFEIFER, J. M. RIGSBEE and K. K. CHAWLA, *J. Mater. Sci.* **25** (1990) 1563.
306. A. P. LEVITT, E. DICESARE and S. M. WOLF, *Metall. Trans.* **3** (1972) 2455.
307. J. K. TIEN and M. W. KOPP, in "Metal and Ceramic-matrix Composites: Processing, Modelling and Mechanical Behavior", edited by R. B. Bhagat, A. H. Clauer, P. Kumar and A. M. Ritter (Metallurgical Society of AIME, Warrendale, PA, 1990) p. 443.
308. B. MARUYAMA, F. S. OHUCHI and L. RABENBERG, *J. Mater. Sci. Lett.* **9** (1990) 864.
309. B. MARUYAMA and L. RABENBERG, *Mater. Res. Soc. Symp. Proc.* 233.
310. M. YANG and V. D. SCOTT, *Carbon* **29** (1991) 877.
311. W. P. MINNEAR, *J. Amer. Ceram. Soc.* **65** (1982) C10.
312. E. FRIZER and R. GADOW, in Proceedings of the International Symposium on Ceramic Components for Engines, 1983, (KTK Science Publishers, Tokyo, 1984) p. 561.
313. T. HASE and H. SUZUKI, *J. Nucle. Mater.* **59** (1976) 42.
314. J. N. NESSE and T. F. PAGE, *J. Mater. Sci.* **21** (1986) 1377.
315. Y. CHIANG, R. P. MESSNER, C. D. TERWILLIGER and D. R. BEHRENDT, *Mater. Sci. Engng* **A144** (1991) 63.
316. M. SINGH and D. BEHRENDT, *ibid* **A194** (1995) 193.
317. A. LI, R. J. ARSENAULT and P. JENA, in "Cast Reinforced Metal Composites", edited by S. G. Fishman and A. K. Dhingra (American Society for Metals, Metals parts, OH, 1988) p. 33.
318. R. ASTHANA, S. N. TEWARI and S. L. DRAPER, *Metall. Trans. A.* (1998) in press.
319. B. J. DALGLEISH, E. SAIZ, A. P. TOMSIA, R. M. CARURON and R. O. RITCHIE, *Scripta Metall. Mater.* **3** (1994) 1109.
320. R. J. KERANS and T. A. PARTHASARTHY, *J. Amer. Ceram. Soc.* **74** (1991) 1585.
321. M. N. KALLAS, D. A. KOSS, H. T. HAHN and J. R. HELLMAN, *J. Mater. Sci.* **27** (1992) 3821.
322. R. ASTHANA, S. N. TEWARI and R. R. BOWMAN, in "High Performance Composites-commonality of Phenomena", edited by K. K. Chawla, P. K. Liaw and S. G. Fishman (Metallurgical Society of AIME, Warrendale, PA, 1994) p. 21.
323. A. S. ARGON, V. GUPTA, H. S. LANDIS and J. A. CORNIE, *J. Mater. Sci.* **24** (1989) 1207.

Received 13 May 1996
and accepted 12 November 1997